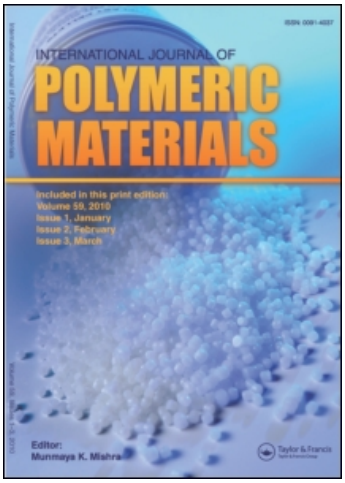

International Journal of Polymeric Materials
Publication details, including instructions for authors and subscription information:
http://www.informaworld.com/smpp/title~content=t713647664

Optical Storage

Thomas Fuhrmann[a]; Joachim H. Wendorff[a]
[a] FB-16-Physikalische Chemie, Universität Marburg, Marburg, Germany

To cite this Article Fuhrmann, Thomas and Wendorff, Joachim H.(2000) 'Optical Storage', International Journal of Polymeric Materials, 45: 3, 621 — 675
To link to this Article: DOI: 10.1080/00914030008035055
URL: http://dx.doi.org/10.1080/00914030008035055

Intern. J. Polymeric Mater., 2000, Vol. 45, pp. 621–675
Reprints available directly from the publisher
Photocopying permitted by license only

Optical Storage

THOMAS FUHRMANN and JOACHIM H. WENDORFF

FB-16-Physikalische Chemie, Universität Marburg,
Postfach, 35032 Marburg, Germany

(Received 18 December 1998)

Digital and holographic optical storage systems are compared. Requirements for the improvement of current storage systems are defined. Techniques to study storage properties of polymer liquid crystals (PLCs) are described; they include diffraction grating, polarization holography, spectroscopic methods, refractive index determination (interferometry, birefringence), methods of surface characterization, and testing reversibility and the number of write-read cycles. Results are reported for several PLCs and interpreted in terms of the effects of the choice of the main chain, the spacer, the chromophore, the LC components, the molecular weight, photoorientation and the surface morphology.

Keywords: Digital optical storage systems; holographic optical storage systems; polymer liquid crystals; PLCs; diffraction grating; polarization holography; spectroscopic methods; refractive index determination; interferometry; birefringence; number of write-read cycles; effects of the choice of the main chain; spacer; chromophore; the molecular weight; photoorientation; surface morphology

1. INTRODUCTION

Since the Audio Compact Disc (CD) was introduced in 1982, the interest in optical storage systems has increased continously. The remarkable success of this new storage medium can be attributed to the combination of two key technologies: the development of a new generation of low-power, miniaturized semiconductor laser diodes and the use of a simple reproduction process, *i.e.*, the injection molding technique of polycarbonate as disc material. These factors allowed mass production and made the CD commercially successful. At the present stage, starting from the CD-ROM (Read-Only-Memory), the

development tends to the realization of storage systems which are optically writable but not erasable (WORM, Write-Once-Read-Many) and to systems which are erasable and rewritable (EDRAW, Erasable Direct Read After Write). A variety of novel materials are currently investigated for these applications, among them PLCs. Thus we begin our discussion with a short overview on currently used materials in order to have a basis of comparison for the capabilities and drawbacks of PLCs as storage media.

1.1. Present Storage Systems

There are two main concepts of optical storage: *digital* and *holographic* storage systems. In *digital* storage systems, the binary encoded information is written bitwise into the 2-dimensional substrate material. The physical property which is changed during the writing process may be reflectivity, refractive index, absorption coefficient, extend of light scattering or magnetization. The materials investigated most frequently for digital storage are shortly summarized in Table I. With respect to rewritable systems (EDRAW), two classes of materials are favoured: magneto-optic and phase-change recording materials. The storage mechanism of the latter is based on a reversible phase change between crystalline and amorphous states of Selen or Tellur alloys, and we will see that this concept is also applicable to order-disorder transitions in PLCs (Section 3.1). A detailed discussion of the various digital storage systems can be found in literature [1–4].

Holographic memory systems are attractive because of the very high storage capacity with short access times. In contrast to digital storage, holographic storage is achieved by recording the interference pattern of the light wave which carries the optical information with a reference

TABLE I Digital recording materials

Photosensitive material	*Storage principle*	*Read-out*	*Type*
Photoresists	master production and replication	Reflectivity	ROM
Dye-in-polymer	ablative writing or bubble forming	Reflectivity	WORM
RE-TM alloys	magneto-optical	MO Kerr effect	EDRAW
Co/Pt multilayers	magneto-optical	MO Kerr effect	EDRAW
Se/Te alloys	phase-change	Reflectivity	EDRAW

wave [5, 6]. The original information can then be reconstructed by illuminating the holographic film with a readout reference beam. Depending on whether the refractive index or the absorption coefficient of the material has been changed, the recorded hologram is called *phase* hologram or *amplitude* hologram, respectively. In general, phase holograms are the better choice because they allow diffraction efficiencies (the percentage of the read-out light that is diffracted into the reconstructed image) of up to $\eta = 1.0$ (100%). For maximal diffraction efficiency, the recording material must be thick in comparison with the wavelength of the writing beams (thick or *volume holograms*). In such volume holographic memories, thousands of holograms may be overlayed by varying the angle or the wavelength of the incident beams, giving rise to a higher storage density. Since there are great progresses in constructing spatial light modulators and detectors for data encoding and retrieving, holographic storage systems seem to be realizable now [7]. But still there is no holographic material available which allows erasing and rewriting.

Today's most common materials for holography are silver halide emulsions derived from photographic recording films, but serious problems arise with the low resolution because of granulation and the need of wet chemical processing. Among the new materials which have been designed to overcome these problems, photopolymers are particularly successful. A concise summary of holographic recording materials is displayed in Table II [6] (for details see Ref. [8]).

1.2. Requirements for New Materials

For the development of new storage systems the following demands have to be considered:

- **Storage Density/Resolution** The theoretical storage density limit for a 2-dimensional memory is $1/\lambda^2$ (10^8 bit/cm^2 for optical wavelengths) and for a 3-dimensional memory $1/\lambda^3$ (10^{12} bit/cm^3). Using special techniques (*e.g.*, spectral hole burning, wavelength and angle multiplexing), the range can be extended to molecular resolution. In existing technological systems, the total capacity of an optical memory disc (5 1/4") exceeded the 1 GByte limit in 1994.
- **Access Times/Data Transfer Rates** Semiconductor devices which are used in computer chips as fast transient memories have access

TABLE II Holographic recording materials

Material	*Spectral range [nm]*	*Exposure [J/m^2]*	*Resolution [lines/mm]*	*Diffraction Efficiency [%]*	*Processing*	*Reusability*
Photographic films	400–700	10^{-3}–10^{0}	1000–10000	5–60	wet chem.	no
Dichromate gelatin	350–580	10^{2}	< 3000	30	wet chem.	no
Photoresists	uv-500	10^{1}–10^{4}	200–1000	10–85	wet chem.	no
Photopolymers	uv-650	10^{0}–10^{2}	5000–10000	50	uv irrad.	no
Photochromics	300–700	10^{0}–10^{3}	5000	1–3	–	yes
Thermoplastics	400–650	10^{-1}–10^{0}	500–1200	10	charge, heat	yes
$LiNbO_3$	350–500	10^{4}	1500	20	–	yes
$Bi_{12}SiO_{20}$	350–500	10^{0}	10000	25	–	yes

times in the range of nanoseconds. The access times of mass memory systems, however, which are designed to have long-time stability, are moderate (up to 10^{-2} s). The effective data access can be optimized by parallelization; attainable data transfer rates are in the range of MByte/s.

- **Wavelength sensitivity** Optical storage systems must be adapted to available laser systems, of which the most preferred are diode lasers (830 nm, 780 nm). The development of low-cost lasers operating at lower wavelengths will be of great importance because it extends the range of photochemical reactions that may be used for the recording process. However, there are many efforts in the field of semiconductor (GaN) and solid-state lasers (Cr : LiSAF) in order to reach blue emission.
- **Exposure energy** The sensitivity curve and the exposure energy required for a sufficient contrast ratio are very important characteristics, especially for holographic recording media. Photochemical processes in organic or polymeric compounds require exposures in the order of magnitude of 10^2 J/m^2, *i.e.*, 10^4 times larger in comparison with photographic films.
- **Reversibility** The reversibility of the photochemical process is crucial for the reusability of the system. The possibility of direct overwriting is preferred to an erasing-rewriting process. Materials suitable for EDRAW should tolerate a number of read/write cycles in the order of magnitude of 10^7.
- **Stability** The stored information should be maintained over a long period, so all types of relaxation processes which eventually lead to partial or complete loss of the data have to be suppressed.
- **Fabrication and Processing** Memory discs or films are produced in large amounts for mass applications, so the simplicity of the production process is of economical interest. The media should be easy to handle, and a post-processing (developing) procedure after the writing process should be avoided.

1.3. PLCs in Optical Storage

Why are polymer liquid crystals so interesting for optical storage applications? Generally, they can combine the mechanical properties

of the PLC matrix with a suitable photochemical system. This offers great advantages with respect to processing properties, stability of the stored information and the possibility of contone recording (grey shade). Up to now, the potential use of PLCs for optical storage has been demonstrated for a series of compounds with different mechanisms, although a technological system has not yet been developed. It turns out that many of the concepts that have been applied successfully to other materials are also applicable to PLCs. The concepts of phase change (Section 3.1) and photopolymerization (Section 3.4) have been applied to PLC materials. Systems with various photochromic organic compounds have been investigated (Section 3.2). But also new ideas for storage mechanisms were developed, for instance a molecular reorientation process by the combination of photoselection and rotational diffusion (Section 3.1). As a unique characteristic feature for a holographic storage medium, the latter system offers the possibility of recording not only amplitude or phase but also the polarization of the writing beam (polarization holography).

Many of the new approaches towards a PLC storage material seem to be very promising for industrial applications, and therefore the interest in these materials goes beyond the pure academic level.

2. EXPERIMENTAL TECHNIQUES

We begin our discussion with a brief introduction into the experimental techniques used for the investigation of the storage properties of PLCs. We mainly focus on the influence of light on the refractive index and the absorption constant, because these are the properties that are important both for holographic and digital applications. In the last section we will cover other properties which may be used as readout parameters in digital storage.

2.1. Characteristic Response Functions

The optical parameter that is influenced by light in the storage process is the complex index of refraction

$$\tilde{n} = n + i\kappa \tag{1}$$

with the refractive index as the real and the absorption constant as the imaginary part.

Since classical optical recording (*e.g.*, photography) is based mainly on the absorption characteristics, the most frequent description of the optical response of a recording medium to the exposure of light is the H&D-curve (Hurter and Driffield, 1890), *i.e.*, the plot of the optical density D *versus* exposure E. The optical density is defined as

$$D = -\log(T) \tag{2}$$

with the *intensity transmittance* of the material

$$T = \frac{I_{\text{out}}}{I_{\text{read,in}}}. \tag{3}$$

whereas the *exposure* is defined as the product of the intensity of the recording beam and the exposure time t

$$E = I_{\text{write}} \cdot t. \tag{4}$$

A typical H & D-curve for a material is shown in Figure 1. Characteristic are three different regions: a certain threshold at the beginning ("toe"), a linear region which should be used for the recording process, and a saturation at higher exposures. The slope of the straight line in the linear region is known as γ value. The whole "gradation" characteristic is given by the first derivative of the $D(E)$-curve

$$g(E) = \frac{d}{dE} D(E). \tag{5}$$

For holographic recording, however, it is more convenient to consider the complex amplitude transmittance

$$t(x, y) = \exp(-\alpha d) \exp(-2\pi i n d/\lambda) = |t| \exp(-i\varphi), \tag{6}$$

where α is the absorption coefficient of the material (proportional to κ), d its thickness and n the refractive index. In practice, the total amplitude transmittance $|t|$ and the phase shift $\Delta\varphi$ are plotted *versus* the exposure E [9]. The two functions correspond to the limiting cases, amplitude modulation (only α varies) and phase modulation (only n varies), respectively.

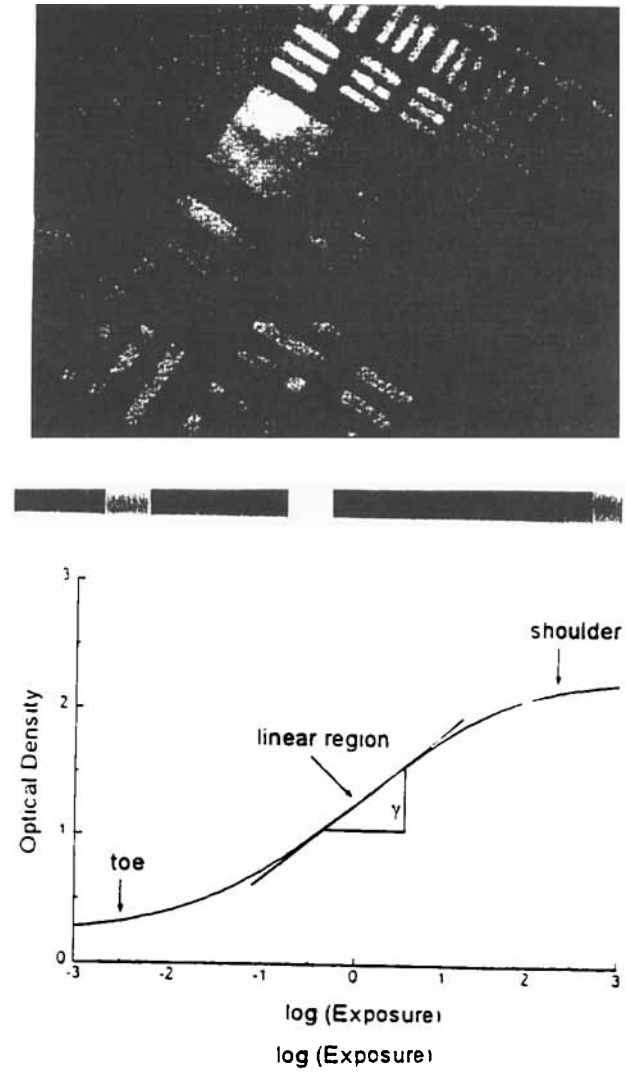

FIGURE 1 A typical H & D curve for a photographic recording material.

A quantity that is often used instead of determining the complete response function is the *inverse sensitivity* measured in J/cm^2. It is defined either as the exposure needed for changing the optical density

by ΔD (by convention, $\Delta D = 0.1$ in ASA and DIN specifications)

$$S_{\Delta D}^{-1} = (I_{\text{write}} \cdot t)_{D_0 + \Delta D} \tag{7}$$

or for obtaining a holographic diffraction efficiency of η (usually 1%), divided by this efficiency

$$S_{\eta}^{-1} = \frac{(I_{\text{write}} \cdot t)_{\eta}}{\eta}. \tag{8}$$

The reciprocity law, *i.e.*, the scaling of the storage parameter (amplitude transmittance or refractive index) with the exposure, is a very important feature and by no means obvious. For simple linear response mechanisms it is valid, but the storage mechanisms in PLCs may show a dependence of the characteristic curves on the writing intensity. However, in most cases the choice of E as the abscissa in the characteristic curves is justified, particularly for low writing intensities.

The curves mentioned above describe the response of the recording material only on a macroscopic scale, but neglect the influences of *microscopic resolution* limits. For this reason, the concept of the *modulation transfer function* (MTF) has been introduced. Its definition is based on the following procedure for sinusoidally varying interference fringes of different spatial frequencies which are recorded in the material, the fringe visibility

$$V = \frac{I_{\max} - I_{\min}}{I_{\max} + I_{\min}} \tag{9}$$

is measured both for the original intensity distribution (V) and for the intensity distribution in the material (V'). The MTF is then defined for any spatial frequency s as

$$\text{MTF} = M(s) = V'(s)/V(s). \tag{10}$$

Because the fringe visibility in the material is less than that of the input pattern due to lateral scattering, the MTF is generally less than unity. For a given material, the MTF may be determined by diffraction methods or microdensitometry (for a review see [9]).

Another method for determining the resolution of the material is the use of test sheets with patterns of different spatial frequencies (Fig. 2) [10].

It may be pointed out that the mentioned characteristic response functions are set up from the applicationer's point of view and cover

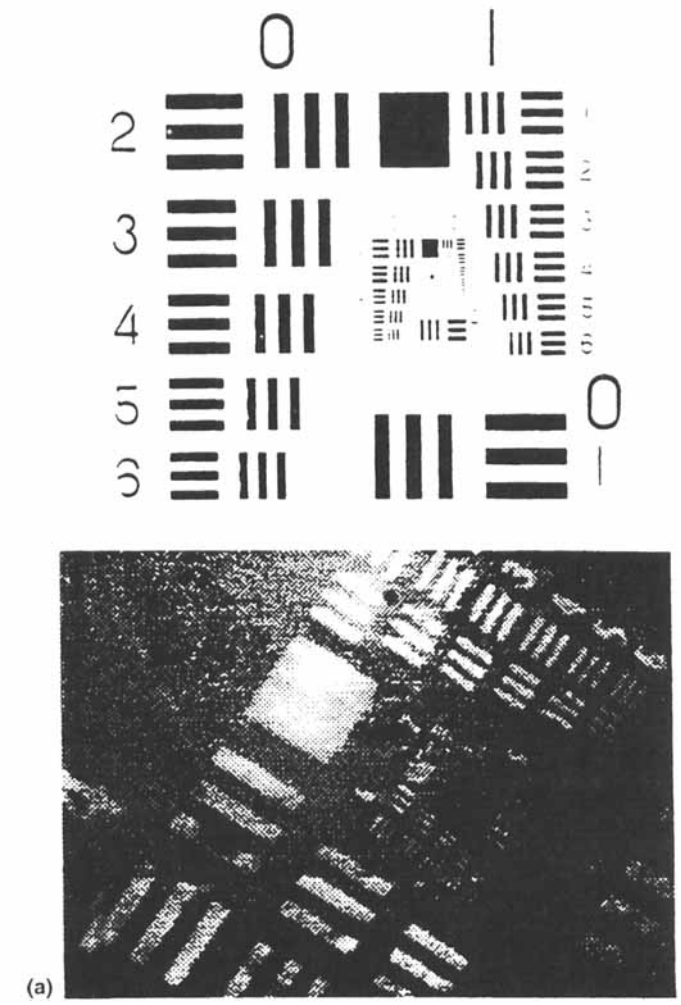

FIGURE 2 (a) US Air Force (USAF) test sheet for determining the resolution of a recording material; (b) Pattern recorded in an azo-dye-containing PLC (viewed between crossed polarizers).

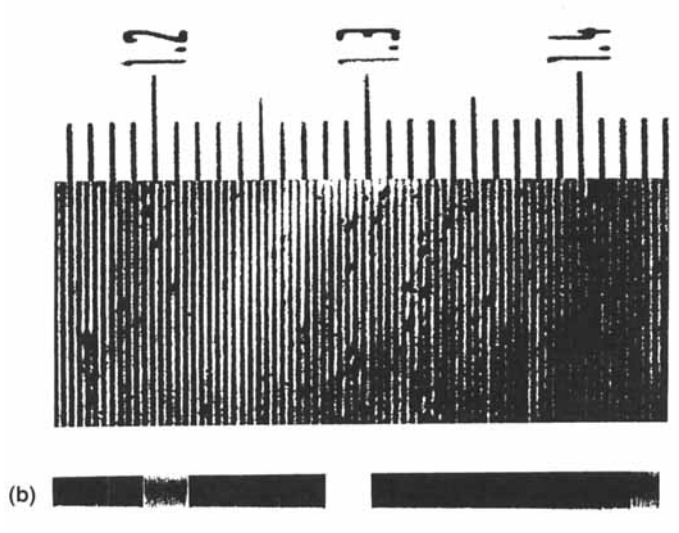

FIGURE 2 (Continued)

the properties of a prefabricated recording film. For a physical characteristic of PLC systems, however, the response functions should be independent of parameters like film thickness, for instance. With respect to this, the plots of transmission and phase change may be replaced by the plots of absorption coefficient α and refractive index n, respectively, as the more appropriate parameters.

Of course, *dichroism* and *birefringence* are very important in PLC systems, so we always have to consider the polarization dependence of light-induced modulations. Thus, the curves $\Delta\alpha(E)$ and $\Delta n(E)$ should be used for characterizing PLC recording materials.

2.2. Holographic Techniques

2.2.1. Diffraction Grating Experiments

There are two reasons why holographic grating experiments are so popular for the investigation of light-induced phenomena in PLCs. First of all, holography is a very sensitive method for measuring

photokinetics by detecting refractive index changes [11, 12]. Secondly, it provides all the important characteristics needed for holographic applications, such as diffraction efficiency and resolution limit.

The basic principle of a diffraction grating experiment [13] is the superposition of two coherent planar waves producing a sinusoidal interference grating (Fig. 3). Depending on the angle between the two beams (2θ) and the laser wavelength λ_{AB}, the grating period is

$$\Lambda = \frac{\lambda_{AB}}{2 \sin \theta} \tag{11}$$

and the intensity distribution along the grating direction (x) is given by

$$\begin{aligned} I(x) &= I_A + I_B + 2\sqrt{I_A I_B} \cos\left(\frac{2\pi x}{\Lambda}\right) \\ &= (I_A + I_B)\left[1 + V \cos\left(\frac{2\pi x}{\Lambda}\right)\right] \end{aligned} \tag{12}$$

with the already mentioned fringe visibility

$$V = \frac{I_{\max} - I_{\min}}{I_{\max} + I_{\min}} = \frac{2\sqrt{I_A I_B}}{I_A + I_B}. \tag{13}$$

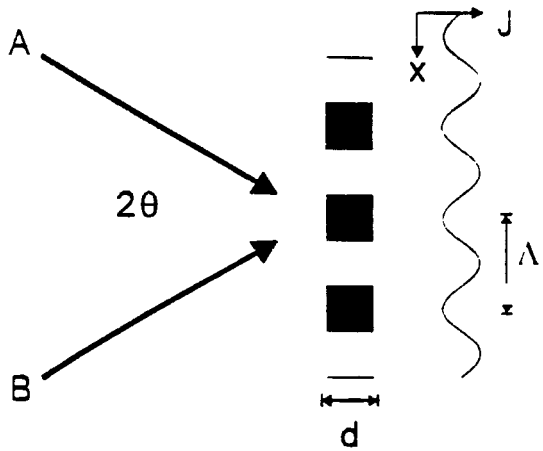

FIGURE 3 Principle of a holographic grating experiment. A sinusoidal grating is formed by the superposition of two writing beams A and B.

Because of photochemical and photophysical processes, both the refractive index and/or the absorption constant of a sample that has been placed into the interference region are modulated with the same spatial frequency

$$n(x) = n_0 + n_1 \cos\left(\frac{2\pi x}{\Lambda}\right) \tag{14}$$

$$\alpha(x) = \alpha_0 + \alpha_1 \cos\left(\frac{2\pi x}{\Lambda}\right). \tag{15}$$

The grating that is written into the sample can be read out (a) by self-diffraction of the writing beams or (b) by a third beam at another wavelength. The latter is preferred because the wavelength of the reading beam can be chosen to be distinct from an absorption line of the material.

In practice, the recording waves are not exactly planar, but have a Gaussian intensity distribution. Therefore, in order to obtain exact results, the probing beam should have a smaller diameter than the spot of the writing beams. Furthermore, for thick gratings (film thickness $d \gg \Lambda$), the angle of incidence must obey the Bragg-condition, *i.e.*,

$$\sin\theta_C = \frac{\lambda_C}{2\Lambda}. \tag{16}$$

The light of the probing beam is diffracted by the grating, and for the efficiency of the first diffraction order, the diffraction formula of Kogelnik is valid [14]:

$$\eta = \frac{I_1}{I_0} = \left[\sin^2\left(\frac{\pi \cdot n_1 \cdot d}{\lambda_C \cos\theta_C}\right) + \sin\mathrm{h}^2\left(\frac{\alpha_1 \cdot d}{2\cos\theta_C}\right)\right] \exp\left(-\frac{2\alpha_0 \cdot d}{\cos\theta_C}\right). \tag{17}$$

If there is no absorption at the wavelength of the probing beam (phase grating), the expression reduces to

$$\eta = \sin^2\left(\frac{\pi \cdot n_1 \cdot d}{\lambda_C \cos\theta_C}\right). \tag{18}$$

Applying this formula, it is in principle possible to determine the light induced refractive index change ($2n_1$) from the diffraction efficiency.

One special extension of Kogelnik's formalism should be mentioned: because of the absorption of the writing beams the refractive index modulation must be modified by a parameter describing the *penetration depth D*. The modulation of the refractive index is then dependent on the z coordinate normal to the sample plane.

$$n(x,z) = n_0 + n_1 \cos\left(\frac{2\pi x}{\lambda}\right) \exp\left(-\frac{z}{D}\right). \tag{19}$$

In that case, the diffraction efficiency becomes [15, 16]

$$\eta = \sin^2\left[\frac{\pi n_1 \cdot D}{\lambda_C \cos\theta_C}\left(1 - \exp\left(-\frac{d}{D}\right)\right)\right]. \tag{20}$$

The evaluation of the hologram growth's curve, however, has certain complications if the intensities of the two writing beams are unequal [17]. It is therefore necessary to adjust a maximal contrast ratio of the grating by making the intensities of the two writing beams equal. A complete experimental setup being used in our group for the investigation of PLCs is shown in Figure 4. The beam from an argon ion laser is divided by a polarization beamsplitter, the intensities in the two arms are adjusted by rotating the first half wave plate. The other half wave plates serve to adapt the polarization directions. By rotating the

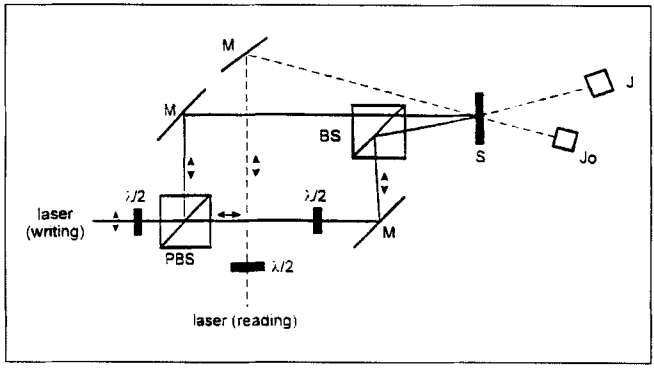

FIGURE 4 Setup for a holographic grating experiment (*M*: mirror, *BS*: beam splitter, PBS: polarizing beam splitter, $\lambda/2$: half wave plate, *S*: Sample).

polarization plane of the read-out-beam, the anisotropy of refractive index change can be measured [18, 19], but normally all beams are *s*-polarized.

Of course, simpler arrangements with slightly different geometries are in use as well.

At this point, a few words should be said about the applicability of Kogelnik's formula. In practice, the conditions which have to be fulfilled for the validity of the formula (*e.g.*, thick gratings) are not given in the experiments. The most serious problem, however, is the existence of *anisotropic* gratings. Here, the coupling between different polarization directions have to been taken into account. The analysis is rather involved and can be done by different methods [20–24].

2.2.2. Polarization Holography

Systems with photoselective excitation mechanisms (Section 3.1) are capable of storing the polarization of the recording lightwave (*polarization holography*). For polarization holography [25–27], the holographical setup is modified as follows: The two writing beams are either linearly polarized with mutually perpendicular polarization directions (a) or left- and right-handed circularly polarized (b) In both cases, the intensity distribution of the interference pattern is constant in the sample plane, but the polarization is modulated in the x-direction (Fig. 5). The experimental setup for type (a) experiments is shown in Figure 6 [28].

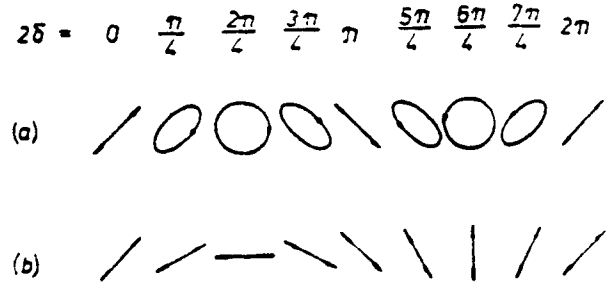

FIGURE 5 Spatial variation of the polarization in a grating formed by (a) two perpendicular linear polarized or (b) two opposite circular polarized waves [27] (reproduced with permission).

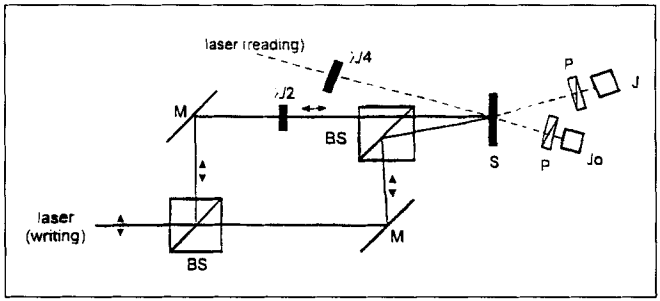

FIGURE 6 Setup for polarization recording (M: mirror, BS: beam splitter, P: polarizer, $\lambda/2$: half wave plate, $\lambda/4$: quarter wave plate, S: sample).

The transmission properties of the polarization hologram can be described with the Jones matrix representation [27, 29]. In a coordinate system (x', y') that is tilted by 45 degrees with respect to the grating direction x, for hologram type (a) the light vector of the interference pattern is

$$E = \begin{pmatrix} E_{x'} \\ E_{y'} \end{pmatrix} = \begin{pmatrix} E_0 \cos\delta \\ iE_0 \cos\delta \end{pmatrix} \tag{21}$$

with

$$\delta = \frac{2\pi \sin\theta \cdot x}{\lambda} \tag{22}$$

and the transmission matrices of the material have the general form

$$\hat{T}_A = \begin{pmatrix} T_0 + \Delta T \cos 2\delta & 0 \\ 0 & T_0 - \Delta T \cos 2\delta \end{pmatrix} \tag{23}$$

for amplitude recording, and

$$\hat{T}_P = \exp(i\varphi_0) \begin{pmatrix} \exp(i\Delta\varphi \cos 2\delta) & 0 \\ 0 & \exp(-i\Delta\varphi \cos 2\delta) \end{pmatrix} \tag{24}$$

for phase recording, respectively.

For hologram type (b) the corresponding expressions are

$$E = \begin{pmatrix} E_0 \cos\delta \\ E_0 \sin\delta \end{pmatrix} \tag{25}$$

$$\hat{T}_A = \begin{pmatrix} T_0 + \Delta T \cos 2\delta & \Delta T \sin 2\delta \\ \Delta T \sin 2\delta & T_0 - \Delta T \cos 2\delta \end{pmatrix} \tag{26}$$

$$\hat{T}_P = \exp(i\varphi_0) \begin{pmatrix} \cos \Delta\varphi + i \sin \Delta\varphi \cos 2\delta & i \sin \Delta\varphi \sin 2\delta \\ i \sin \Delta\varphi \sin 2\delta & \cos \Delta\varphi - i \sin \Delta\varphi \cos 2\delta \end{pmatrix} \tag{27}$$

For isotropic media it turns out that

- in type-(a)-holograms the polarization of the read-out beam influences the polarization of the diffracted wave but not the efficiency
- whereas in type-(b)-holograms the polarization of the read-out beam influences the efficiency but not the polarization of the diffracted wave.

In materials with intrinsic birefringence, however, as PLCs are the phase difference between ordinary and extraordinary waves in z-direction

$$\Delta(z) = \frac{2\pi(n_1 - n_2)z}{\lambda} \tag{28}$$

has to be considered. This means that the modulation shape varies along the depth of the material, resulting in a mixture of linear polarization grating (type (a)) and circular polarization grating (type (b)) (see Fig. 7). Nikolova and Todorov showed that the diffraction efficiency depending on the read-out polarization angle α may be expressed as

$$\eta_{\pm} = \frac{\Delta T^2}{4} \begin{pmatrix} 1 + \left(\frac{1-\cos 2\Delta}{4\Delta}\right)^2 \\ + \frac{(1-\sin c(2\Delta))^2}{4} \pm (1 - \sin c(2\Delta)) \sin 2\alpha \end{pmatrix} \tag{29}$$

with an average phase shift Δ [27]. Because of the superposition of different gratings, the mathematical description of these phenomena is quite complex [30], so most of the investigations have been done only qualitatively.

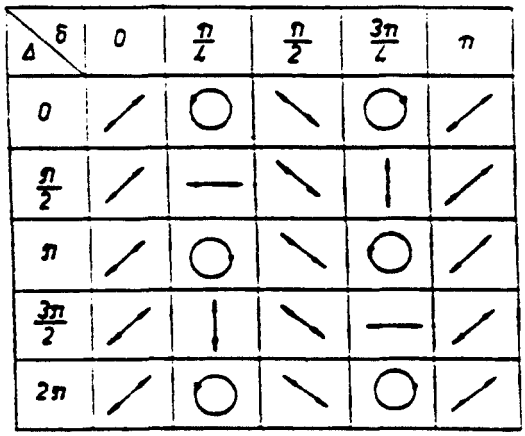

FIGURE 7 Spatial variation of a type (a) polarization grating parallel and normal to the sample plane [27] (reproduced with permission).

2.3. Spectroscopic Methods

It was pointed out in the preceding section that holographic methods are sensitive both to changes in the refractive index and in the absorption constant. With spectroscopic methods, the photochromic properties of the storage materials (*i.e.*, the change of absorption when the sample is irradiated) and the dichroism can be extracted.

A spectroscopic investigation of optical response behaviour involves two lights sources: one for the writing process, and another for probing the sample. In most cases, the writing beam is a laser in the visible or near-infrared region, whereas the probing light, depending on the chemical species that has to be monitored, may be visible (for chromophores), UV- (for mesogenic aromatic units *e.g.*, biphenyles, esters, amides) or IR-radiation (for special substituents *e.g.*, cyano or hydroxyl groups). In order to suppress an influence on the recording process, the intensity of the probing light should be weak compared with the writing beam intensity.

Polarization spectroscopy is necessary for two reasons: First, in an oriented PLC, the anisotropy of the liquid crystalline phase provides an intrinsic polarization dependence of the optical properties. Secondly, the use of polarized writing beams induces an additional uniaxial anisotropy because of photoselection.

A typical setup for UV polarization spectroscopy with time-resolved recording is drawn in Figure 8, a similar setup may be used for IR measurements. The linear dichroism

$$L.D. = \frac{E_{\parallel} - E_{\perp}}{E_{\parallel} + E_{\perp}} \tag{30}$$

is obtained by measuring the absorbances at different polarization angles.

Higher precision and time resolution can be obtained by *modulation polarization spectroscopy*. Here, the rotating polarizer is replaced by a fixed polarizer and a photoelastic modulator oriented with its principal axis at 45 degrees with respect to the polarizer. By modulating the birefringence of the photoelastic device, the state of polarization is changed. The signal is recorded by a lock-in-amplifier, measuring the intensity $I_{\parallel} - I_{\perp}$, and a DC integrator, measuring $I_{\parallel} + I_{\perp}$, respectively (Fig. 9).

Since the underlying principles of spectroscopy with polarized light and its applications are reviewed comprehensively [31, 32], we will only sketch the theory for the evaluation of order parameters from dichroism measurements:

Almost all of the storage mechanisms in PLCs are based on (or at least can be detected by) a change in the molecular orientational distributions. Therefore we need a description of the ordering state in

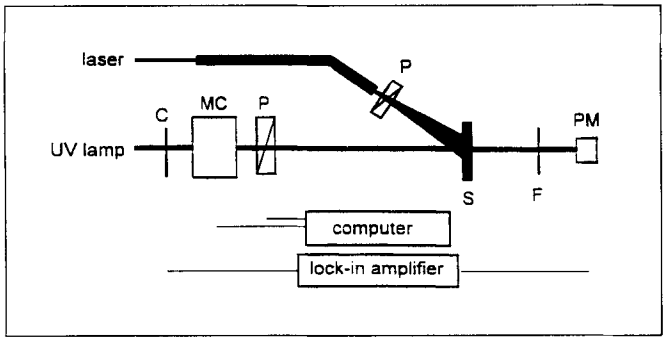

FIGURE 8 Setup for an UV polarization experiment (*C*: Chopper, *MC*: monochromator, *P*: polarizer, *S*: sample, *F*: bandpass filter, *PM*: photomultiplier).

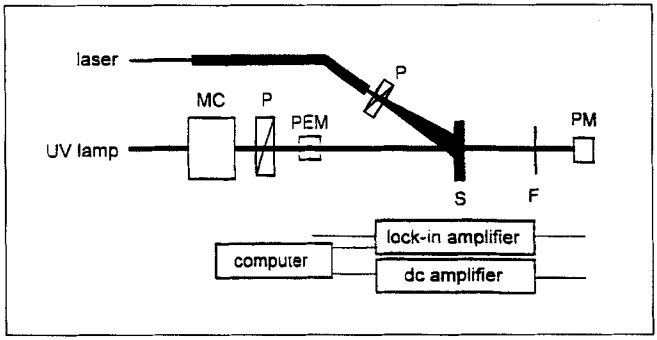

FIGURE 9 Setup for a modulated UV polarization experiment (*MC*: monochromator, *P*: polarizer, PEM: photoelastic modulator with a time-varying retardation of $\pi\sin\omega t$, *S* : sample, *F*: bandpass filter, *PM*: photomultiplier). The lock-in amplifier operates at the double frequency 2ω.

the PLC. There are three interchangeable sets of parameters describing orientation anisotropy: Orientation factors, Saupe order parameters and Wigner matrices. Here we adopt the orientation factor representation for uniaxial as well as biaxial samples, because we will use it later on when we are discussing photoselectivity.

The internal coordinate system of a molecule (x, y, z) in the sample can be related to the laboratory system (X, Y, Z) by defining angles between all the axes (represented by direction cosines). In an absorption experiment using linearly polarized light along Y (with propagation direction Z), the transition probability of a single molecule is related to the square of its transition moment (only one transition in z is supposed):

$$M_Y^2 = [M_z \cos(z, Y)]^2. \tag{31}$$

Averaging over all molecules and defining the orientation factors for the three laboratory coordinates $i = X, Y, Z$

$$K_{zi} = \langle \cos^2(z, i) \rangle, \tag{32}$$

We obtain

$$\overline{M_Y^2} = M_z^2 \cdot K_{zY}. \tag{33}$$

In uniaxial samples, the transition probability for perpendicular (X) polarized light would be

$$\overline{M_X^2} = \frac{1}{2}[M_z^2(1 - K_{zY})]. \tag{34}$$

In an isotropic sample, all K_{zi} would be equal (1/3, 1/3, 1/3), and for perfect alignment along Y they are given by (0, 1, 0). In all cases they must sum to give unity:

$$K_{zX} + K_{zY} + K_{zZ} = 1 \tag{35}$$

The absorbances $E_{\parallel} = E_Y$ and $E_{\perp} = E_X$ can be used for calculating the orientation factors. Assuming that we have one transition with a transition moment along z, the orientation factor for a uniaxial distribution (*e.g.*, induced by photoselection under Y-polarized light) in Y would be

$$K_{zY} = \frac{E_Y}{2E_X + E_Y}. \tag{36}$$

It is possible to transform the orientation factors into Saupe parameters

$$s_{zY} = \frac{1}{2}(3K_{zY} - 1), \tag{37}$$

and the order parameter of uniaxial samples becomes

$$s_{zY} = \frac{E_Y - E_X}{E_Y + 2E_X} \tag{38}$$

in terms of polarized spectroscopy.

2.4. Refractive Index Measurements

As dichroitic measurements are necessary for characterizing photochromism in anisotropic samples completely, refractive index measurements have to include the determination of birefringence. For measuring changes in the refractive index, there are many experimental methods which may be used instead of or in combination with holographic grating experiments (Fig. 10).

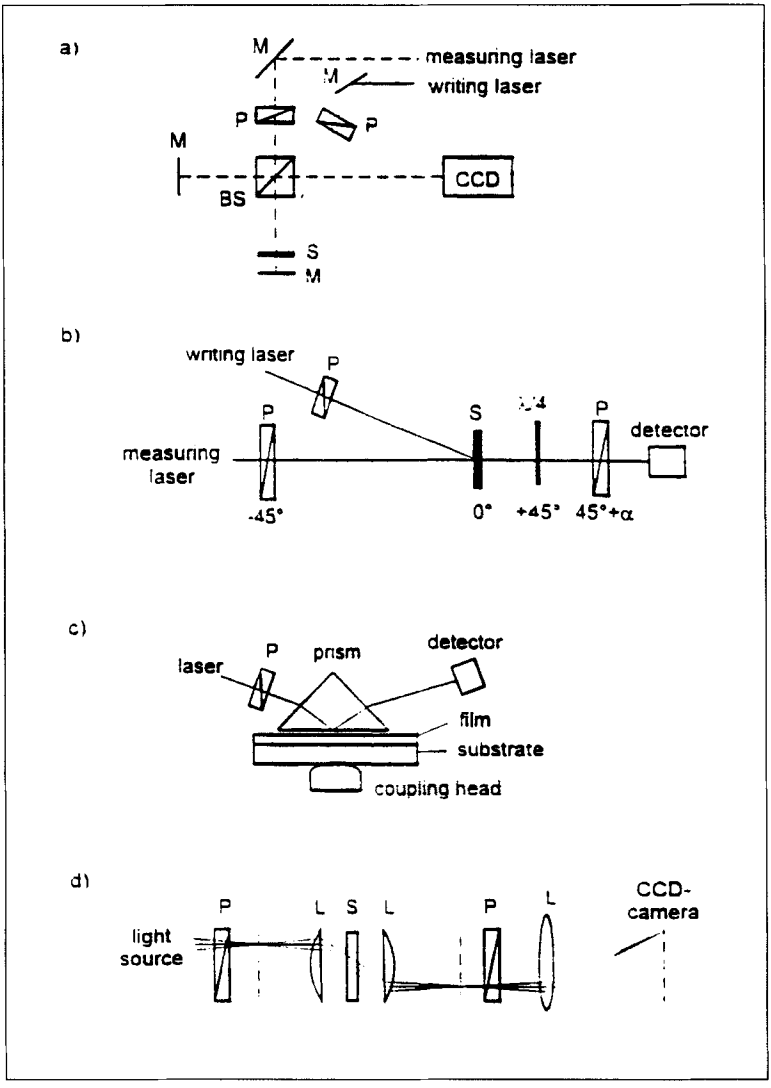

FIGURE 10 Different methods for measuring refractive index and birefringence: a) Michelson interferometer; b) translation into amplitude modulation by crossed polarizers; c) prism coupling method; d) the basic principle of conoscopy: interference patterns for different incidence angles are imaged (*M*: mirror, *P*: polarizer, *S*: sample, *L*: lens).

(a) Interferometry

The sample is placed in one arm of a Michelson or Mach-Zehnder interferometer where it can be irradiated by an external light source [33]. Observing the interference intensity, changes of the optical path length can be measured directly. This method is well suitable for online-measurements.

(b) Birefringence Measurements

The classical method for measuring changes of birefringence is the translation of phase changes into amplitude changes by positioning the sample between crossed polarizers. If the optical axis of the PLC is oriented at 45 degrees with respect to the axes of polarizer and analyzer, the transmitted intensity is given by

$$J = J_0 \sin^2\left(\frac{\delta}{2}\right) \tag{39}$$

with the retardation

$$\delta = \frac{2\pi \cdot \Delta n \cdot d}{\lambda} \tag{40}$$

from which the birefringence Δn can be calculated.

A higher sensitivity can be achieved in a slightly modified arrangement that is frequently used also in Kerr experiments [34]. In this modified setup a quarter-wave plate with its slow axis perpendicular to the polarizer is placed behind the sample, and the analyzer is tilted by a defined angle α. Here, the transmitted intensity is

$$J = J_0 \sin^2\left(\alpha + \frac{\delta}{2}\right) \tag{41}$$

It can be shown that the amplitude of intensity variation is increased in comparison with the unmodified setup [35]. A second advantage of this method is that the sign of refractive index change can be determined. In certain cases, if the direction of the optical axis of the sample is not known, the sample may be fixed on a rotating stage [36].

In another variant of the setup, the analyzer is replaced by a polarizing beam-splitter, and the signals in both polarization directions are measured independently by two photodiodes.

(c) Prism Coupling Method

The PLC film on a substrate is brought into contact with a prism, and an incending laser beam is reflected at the prism-PLC interface. At certain angles of incidence, waveguide modes are excited in the polymer, and the intensity of the reflected light decreases. From the (angular) distance of these modes, film thickness and refractive index can be determined with high accuracy [37]. Although this method is less suitable for time-dependent measurements, it very sensitive and allows the determination of the absolute values for the refractive indices in all three directions (by TE and TM mode analysis) [38]. New approaches combine the prism coupling method with the diffraction grating technique using a two-beam geometry [39].

(d) Polarizing Microscopy and Conoscopy

By these methods, the direction of the optical axis can be determined. In contrast to (orthoscopic) polarizing microscopy, conoscopic imaging leads to the interference patterns for different directions in the sample, and allows the determination of an optical axis perpendicular to the sample. Recently, setups with high spatial resolution (scanning conoscopy [40]) have been developed.

2.5. Methods for Surface Characterization

Many of the storage mechanisms influence the *surface morphology* of the PLC. For the characterization, *electron microscopy* (SEM and TEM) or *atomic force microscopy* (AFM) may be used, for instance. However, of special importance with respect to *optical readout* are techniques like *optical reflectometry* or light scattering experiments. As mentioned in the introduction, digital storage applications are not limited to the readout of absorption or birefringence, but reflection and scattering properties may also be used as read-out parameters. A digital read out system measuring the reflectivity of the PLC surface would resemble the conventional Compact Disc read-out technology (Fig. 11), so a similar arrangement may be used for testing. Moreover, changes in

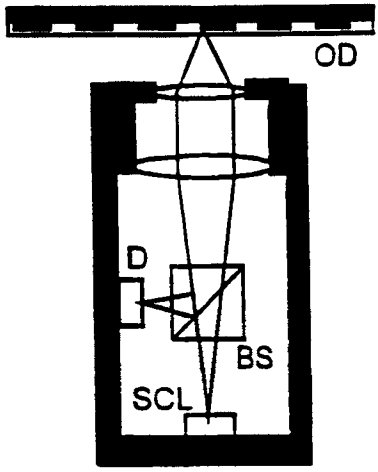

FIGURE 11 Cross-section of a typical disc player with optical readout by reflection from the disc surface (*OD*: optical disc, *BS*: beam splitter, SCL: semiconductor laser, *D*: detector).

the polarization state of the reflected light which are a direct result of modified birefringence can be analyzed by *ellipsometry* [41]. The possibility of optical readout by *surface plasmon microscopy* which is based on the prism coupling method was also demonstrated for PLC films [42].

2.6. Testing Reversibility and Number of Write-read Cycles

In order to complete the characterization of materials for erasible storage applications, the degree of reversibility after many write-read cycles has to be determined. This can be done, for instance, by a method adapted from WORM disc technology [43]. The writing beam is modulated as a random bit stream (0 and a 1) in that way that a writing pulse means the transition from 0 to 1 and a erasing pulse the transition from 1 to 0. The transitions 0 to 0 and 1 to 1 require no writing intensity. If the readout data are superimposed and grouped in sets of three bits, the result is a so called 'eye diagram' (Fig. 12). Its shape represents the superposition of all eight combinations of a three bit data set (000, 001, 010, 011, ...). A decreasing of the distance

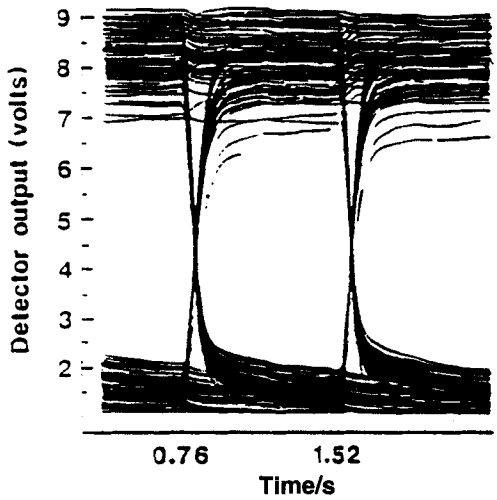

FIGURE 12 "Eye diagram" for the 3-bit superposition of 500 write-erase cycles in a polymer liquid crystal [43] (reproduced with permission).

between the '0' and '1' levels after many write-read cycles indicates fatiguing of the material. The maximum sampling frequency is reached when the transition curves become blurred. Of course, the principle can be extended from binary to n-level coded data, giving information on grey scale possibilities [43].

3. PLC MATERIALS

3.1. Phase-transition-recording

3.1.1. Thermooptical Recording

The first demonstration of optical storage in PLCs was published in 1983 by Shibaev *et al.* [44]. The storage concept is based on a *thermooptically induced phase transition* between the mesophase and the isotropic melt. The concept of phase-change recording with PLCs actually resembles the storage process in phase-change alloys, and, of course, it has been applied to MLCs as well [45].

In order to prepare the PLC in Figure 13 for the writing process, it was oriented homeotropically in an electrooptical cell by applying an AC electric field and kept a few degrees below the clearing temperature.

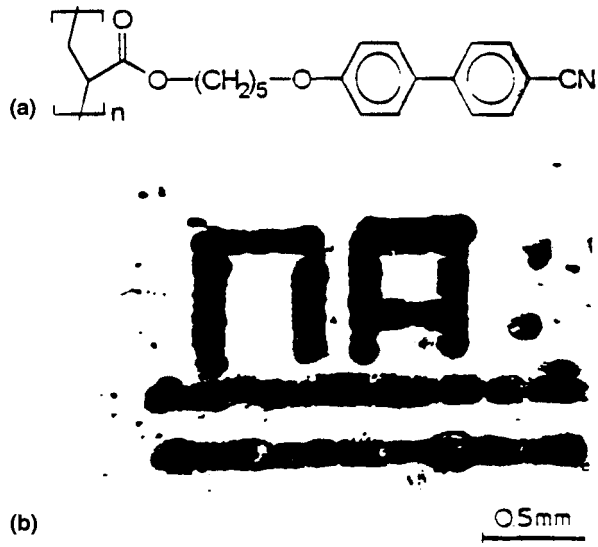

FIGURE 13 (a) The first PLC optical recording material: a polyacrylate with cyanobiphenyl side chains; (b) stored test pattern, obtained by thermorecording with a HeNe laser beam [44].

Local heating by the writing beam of a HeNe laser causes a transition to the isotropic melt, and the homeotropic orientation is destroyed. On cooling, a polydomain texture that scatters light is formed (Fig. 14). Erasing can be done by applying the electric field again.

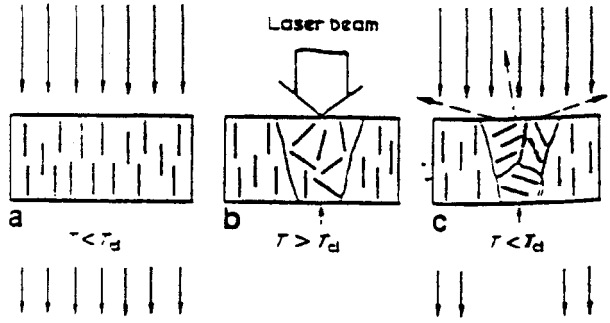

FIGURE 14 The principle of thermorecording: local heating causes a nematic–isotropic phase transition, which leads to scattering microdomains after recooling [44].

The great advantage of phase-transition recording in PLCs in comparison with MLC's is that the orientation relaxation rate of the domains is very low below the glass transition temperature, so the written information can be stored for a long time when the film is kept below T_g.

Using polysiloxanes with *p*-cyanobiphenyl side chains, Coles and Simon showed that this type of recording can also be done at room temperature with smectic PLCs [46]. The storage properties of similar polymers with *p*-cyanophenylbenzoate side chains have been investigated in detail by McArdle *et al.* [47].

In order to increase the thermal absorption of the polymer film, *guest dye molecules* can be dissolved in the host PLC [46, 47]. These dyes are adapted to the writing wavelength (*e.g.*, blue antraquinone dyes for absorbing at the 633 nm HeNe laser line). Using laser pulses of 300 μs, write-in and selective erasure times were on the submillisecond time scale. The sensitivities were determined to be $12 \cdot 10^3$ J/m^2 [47].

The sensitizing dyes can also be incorporated into the side chains of the PLC. Copolymers with 36 wt.-% anthraquinone dye content still show nematic phases, although the nematic to isotropic transition is substantially lowered [48].

Main chain LC polycinnamates were investigated as well, but here the phase transition effect is accompanied by crosslinking rearrangement reactions, so the process is irreversible [49].

An erasable optical memory with cholesteric PLCs was demonstrated by Nakamura and Ueno [50, 51]. They used 0.6 – 30 μm thick films of oligosiloxanes with cholesterol and biphenyl moieties as the recording material. The films were annealed to obtain a planar texture. A 830 nm laser diode was used for recording with 30 μs pulses. Here, the storage effect is measured rather in reflection than in transmission mode, detecting changes in the cholesteric reflection of circular polarized light. As in the case of nematic and smectic PLCs, thermooptical heating above the clearing temperature causes light scattering microdomains when the film is cooled down again. But in addition, a color shift from red to green in the cholesteric reflection was observed, indicating a decrease of the helical pitch due to the heating (Fig. 15).

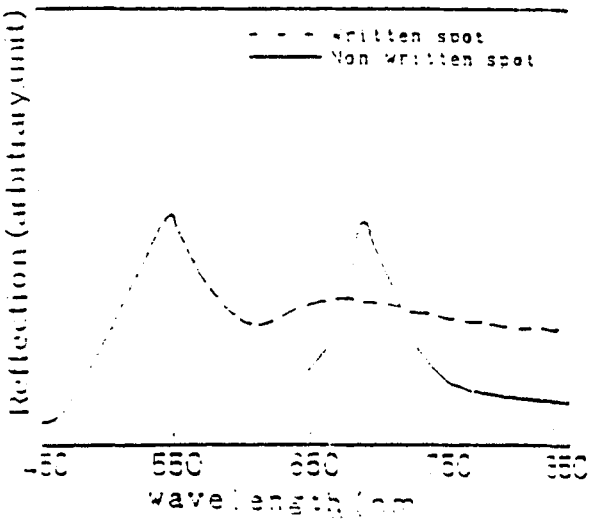

FIGURE 15 Change in cholesteric reflection of left circular polarized light for a cholesteric polysiloxane which has been irradiated at 830 nm [51] (reproduced with permission).

3.1.2. Photoinduced Phase Transitions

In contrast to the previous storage principles, "photon mode" recording is based on photochemical processes in the PLC and not on heating effects. All photochromic and orientable systems that are described in Sections 3.2 and 3.1 fall into this category, and the first "photon mode" system was introduced by Eich and Wendorff in 1987 (see Section 3.1) [52, 53]. Here, only those systems are treated which exhibit a *photochemically induced phase transition* that can be used for optical storage.

Two different types of PLCs were examined by Tazuke and coworkers: (i) polyacrylates with *p*-methoxyphenylbenzoate side chains, doped with 4-butyl-4′-methoxy-azobenzene and (ii) copolymers with the azobenzene moiety incorporated into the side chains (Fig. 16) [54, 55]. The mesophases of these PLCs are destroyed by the photochemical *trans-cis*-isomerization of the azobenzene (Fig. 17). Nematic alignment is favoured for the rodlike *trans*-isomer, whereas the "bent" *cis*-isomer being produced upon irradiation at 366 nm leads to a disturbance of the orientation. Therefore a isothermal phase transition

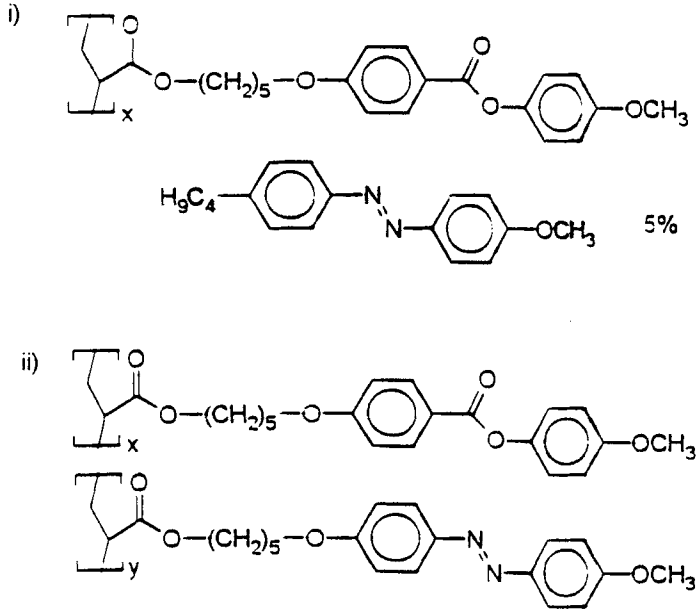

FIGURE 16 PLCs containing azo chromophores for isothermal phase-transition recording [54, 55].

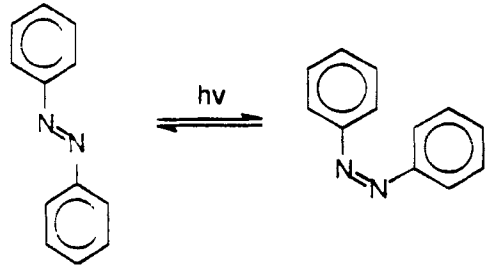

FIGURE 17 *Cis-trans* isomerization of azobenzene. The geometry of the molecules changes from a rodlike to a bent shape.

to the isotropic phase is observed, resulting in the complete loss of birefringence. The initial state can be recovered photochemically by irradiation with visible light (525 nm). For long-term storage, however, the rapid thermal *cis-trans*-conversion (50% of the molecules are back in the *trans* state after 15 min at 58°C) can be suppressed by cooling the polymer below T_g. The phase transition behaviour was found to be strongly dependent on the spacer length and the molecular weight of

the PLC. By calorimetric studies and order parameter determinations it was shown that the efficiency of the photoinduced phase transition is higher in systems with less ordered nematic states (these are the systems with a high content of azobenzene). PLCs containing *p*-cyanobiphenyl mesogens, however, show the important difference that in the latter system a higher content of azobenzene does not weaken the interaction of the mesogenes and therefore does not make the transition easier [56]. Generally, phase transition in PLCs proceed slower than in guest-host-mixtures of azo dyes and MLC's [57], but this problem can be solved by preparing ternary mixtures of an azobenzene derivative. MLC and PLC [58, 59].

Very interesting is a new approach of connecting the azo chromophore non-covalently *via* hydrogen-bonds to the polymer backbone. Isothermal nematic–isotropic phase transitions were observed by irradiating such a supramolecular complex with UV or visible light [60].

Phase transitions also occur in PLCs with spiropyran groups, but since in this case the more important feature are the photochromic properties, these systems will be covered in Section 3.2.

3.1.3. Photo-induced Change of Cholesteric Order

Pinsl *et al.*, presented a system that is based on the *photochemical destruction of helical order* in cholesteric oligosiloxanes (Fig. 18) [61]. The benzophenone chromophore is either covalently attached to the oligosiloxane ring or used as a dopant. The cholesteric reflection band at 500 nm disappears under irradiation at 351 nm because of an irreversible photoreaction between the additive and the cholesterol groups. The storage system may have data rates of 100 MHz and exhibits a high contrast in reflectivity, but its important disadvantage is the lack of reversibility. Using carbon black instead of benzophenone as a dopant expands the spectral sensitivity over a wide range up to the near infrared region. Because of a sharp threshold in the writing sensitivity, non-destructive reading is possible with a beam of low intensity.

A related system consists of a PLC doped by an isomerizable chiral dye which induces a cholesteric phase. By UV irradiation, a color shift of the cholesteric reflection was observed [62].

Another method of detecting the structural changes in cholesteric systems was shown recently: the LC-induced circular dichroism of an

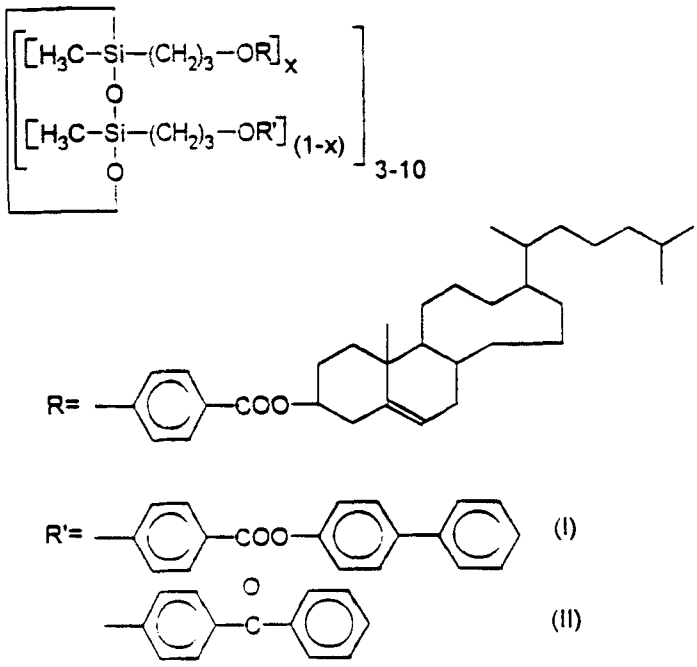

FIGURE 18 Cholesteric polysiloxane with benzophenone moieties used for irreversible recording [61].

anthraquinone dye doped in a cholesteric PLC can be switched reversibly if azo dye molecules are incorporated into the system. The effect was explained by an orientational change of the anthraquinone groups being influenced by the photoisomerization of the azo dyes [63].

All phase-transition materials require a certain threshold intensity in the writing process. Thus writing and reading can be done with the same laser source which is very important for technological PLC storage systems [64].

3.2. Photochromic Systems

Photochromic systems allow optical switching between two (or more) molecular states with different absorption characteristics. The reversibility of these systems is of special interest for erasable storage media. Nevertheless, the states should be stable with respect to thermal

interconversion, and selective switching from state 1 to state 2 with light of a certain wavelength and from state 2 to state 1 with light of another wavelength should be possible.

$$A \leftarrow B$$

The chemical realization of various types of photochromic systems that may be used involves electron transfer reactions, isomerizations and photocyclizations [65]. When investigating PLCs containing a photochromic moiety, it must generally be taken into consideration that the structure of the mesophase is coupled to the photochromic effect (Section 3.1). Additionally, there may be orientational order effects due to photoselection (Section 3.1).

3.2.1. Spiropyrane-containing PLCs

Photochromism in spiropyranes is based on a ring opening reaction of the spiropy-rane to the merocyanine form (Fig. 19) by irradiating with UV light. The merocyanine form is coloured ($\lambda_{max} \approx 580$ nm) and can be transformed back to the transparent spiropyrane by irradiating with visible light. At higher temperatures a third, red-coloured species is formed which can be attributed to aggregated dimers of the merocyanine. Such H-aggregates are favoured because of the large change in the molecular dipol moment due to the charge separation in the isomerization step. The photochromic properties of various acrylate and silicone copolymers with the spiropyrane moiety either linked at one end of the molecule (rod-shaped) or *via* the pyrrolidine amino function (T-shaped) have been investigated [66–68].

The problems of spiropyrane systems are the thermochromic behaviour which may interfere with the photochromic property, the low kinetic stability of the merocyanine form with respect to the

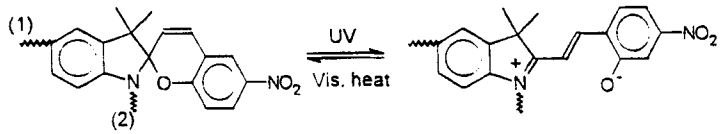

FIGURE 19 The interconversion of spiropyranes to the coloured merocyanine form. The chromophore may be attached at position (1) or (2) to the polymer main chain.

backisomerization and the possibility of photochemical side reactions. In PLCs, however, the merocyanine form is stabilized by the liquid crystalline order, the formation of aggregates and solvatochromic effects. The backisomerization does not follow first-order kinetic, but it has a fast first order component which can be estimated to be about $10^{-6}\,s^{-1}$ [67].

3.2.2. Fulgimide-containing PLCs

A very promising system has been developed by Ringsdorf and coworkers [69], because it does not show any thermochromism: in contrast to other photochromic systems the energetically higher form cannot relax thermally. The switching process is the electrocyclical ring closure of a fulgimide, yielding 7,7a-dihydro-benzofurane (Fig. 20)

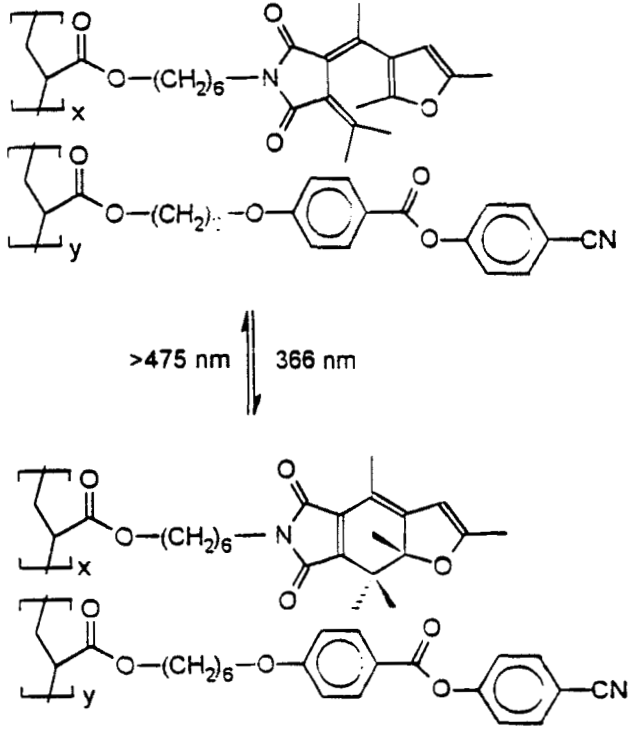

FIGURE 20 The ring closure reaction of fulgides which are incorporated in PLCs [69].

Whereas the photoreaction is induced at 366 nm, the back reaction requires visible light [70]. The written information was shown to be stable even above T_g, no change in absorption had been observed when the film was kept in the dark for 300 h.

3.2.3. "Reverse Mode" (Biphotonic) Mechanisms

All photochromic systems which show bistability may be used in the "reverse mode", *i.e.*, first the whole film is irradiated to pump the molecules into the higher state, and then the information is written by inducing the back reaction. Of course, the relaxation rates remain the same, but this procedure may have advantages when the back reaction is induced with photons of low energy. So in the case of spiropyrans, holography could be performed at 514 nm instead of 365 nm [68]. For PLCs with azo benzene side chains, a "biphotonic" storage was reported [71], based on a previous irradiation at 488 nm and subsequent holographic grating formation at 633 nm. This behaviour could be explained with a red-photon-induced transition from the *cis* to the *trans* isomer [72, 73]. The process can be distinguished from a thermally induced isomerization by its dependence on the wavelength and the polarization plane of the writing light.

These biphotonic mechanisms are different from processes which involve transient molecular states. The latter have been the subject of many investigations, and optical storage with these materials at near-IR wavelengths has been proposed [11].

3.3. Orientable Systems

A new storage concept was introduced by our group in 1987. The storage principle is a reorientation of the optical axis in uniaxial oriented PLCs. Although it uses a reversible photoreaction, it differs from photochromic storage because the stability of the written information does not depend on the relaxation of the energetically higher molecular state but on the rotational diffusion characteristics in the liquid crystalline domain. As an important property for this type of storage it should be emphasized that writing can be done even in the glassy state.

3.3.1. Photoselection

The storage principle is based on the photoselective property of a dichroic dye molecule. Because of the anisotropy of the molecular transition moment, the probability of excitation depends strongly on the orientation of the dye molecule. According to the basic laws of photochemistry, this dependence is given by

$$W \propto M_Y^2 = M_z^2 \cos^2(z, Y) \tag{42}$$

with the definitions given in Section 2, and assuming that only a transition moment in the molecular z-direction contributes to the excitation. Thus, when irradiated with Y-polarized light, only those molecules are selected which have the "right" orientation. If the excited molecules undergo a photoreaction, an additional anisotropy is induced by this photoselection.

For an isotropic sample, the initial orientation factors of the *transformed* molecules after the irradiation would be

$$K_{zY} = \frac{3}{5}; K_{zX} = K_{zZ} = \frac{1}{5} \tag{43}$$

indicating an uniaxial distribution. With progressing irradiation, photoselection no longer occurs from a random sample, and after an infinite time all molecules are transformed.

The corresponding expressions for an anisotropic sample are more complex, because they depend on the angle between polarization plane and the optical axis of the sample, for instance.

Photoselectivity means that the polarization direction of the writing light can be stored within the sample. Thus all photochromic materials are in principle suitable for polarization recording (Section 2). For the reorientation process, however, a second step must be introduced.

3.3.2. The Storage Principle

A special case in photoselective systems arises when the photoreaction is reversible. This is the case for azobenzene derivatives. Figure 21 sketches the absorption spectra of *trans* and *cis* azobenzene: they both exhibit a strong absorption band around 350 nm ($\pi\pi^*$-transition) and a small

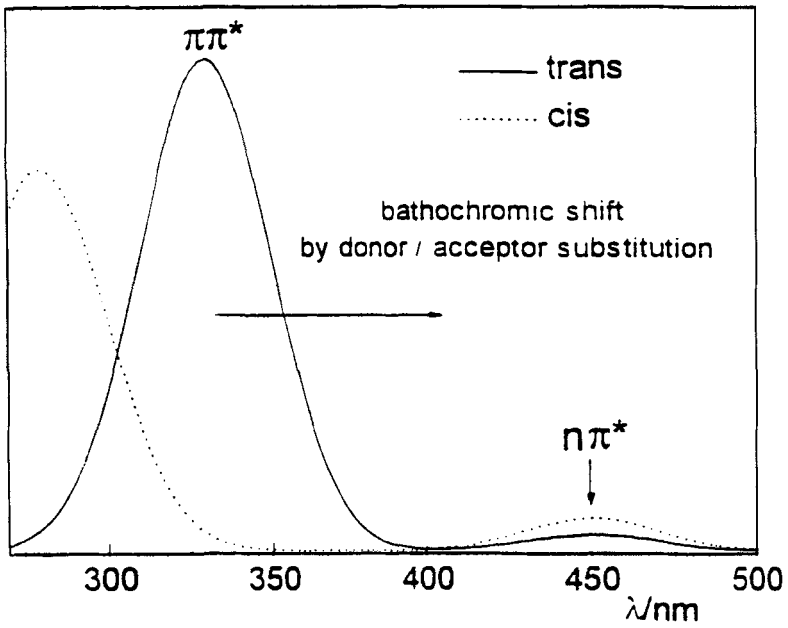

FIGURE 21 Absorption spectra of *trans*- (solid line) and *cis*-azo dyes (dashed line).

band at 450 nm ($n\pi^*$-transition). Irradiation of either of the bands leads to the isomerization reaction, but with different reaction paths ($\pi\pi^*$-transitions probably prefer a rotational. $n\pi^*$-transitions an inversion isomerization mechanism). The spectra of the isomers overlap, that means that both reactions take place in solution, leading to a photostationary equilibrium. The third reaction that is involved is the thermal backisomerization, which shifts the equilibrium to the *trans* side at higher temperatures. Because of different quantum yields and extinction coefficients [74], the equilibrium between *trans* and *cis* is strongly dependent on the irradiating wavelength. In general, $\pi\pi^*$-excitations lead to higher *cis*-concentrations in the photostationary state. Phase transition recording with azo dyes (Section 3.1) uses the high *cis* concentration under UV irradiation for the distruction of the liquid crystalline order. For the reorientation mechanism, however, a *low cis concentration* in the photostationary state, but *high isomerization rates* are preferred. In this case, irradiation of the $n\pi^*$-band is the better choice.

Because of the simultaneous excitation of *trans-cis-* and *cis-trans* isomerization, the molecules undergo *isomerization cycles*. In each isomerization step they are able to change their orientation in the matrix ("*photoinduced rotational diffusion*"). Finally, they tend to orient perpendicular to the polarization plane of the light, because in that orientation they will not be excited again and can no longer take part in the isomerization cycle. So the overall effect is a reorientation of the molecules. The new orientation distribution would be disclike in a plane that is normal to the polarization direction (Y), with orientation factors

$$K_{zY} = 0; K_{zX} = K_{zZ} = \frac{1}{2} \tag{44}$$

In liquid crystalline systems, this process is in competition with the liquid crystalline order, leading to biaxial ordering states. The effect that can be seen experimentally is a realignment of the optical axis, as it is demonstrated in Figure 22 for a nematic side chain homopolymer with azo chromophores. After a longer time of irradiation, the optical axis is rotated to an angle of 90° with respect to the polarization plane of the writing light. The decrease of absorption is mainly due to a tilting of the director into the Z-direction (normal to the sample plane) or due to *cis*-isomers which have not been transformed back.

A mathematical treatment of the reorientation process is rather involved. One approach uses differential equations for the time-dependence of the orientation functions $f(\Omega)$ for both isomers [28, 75].

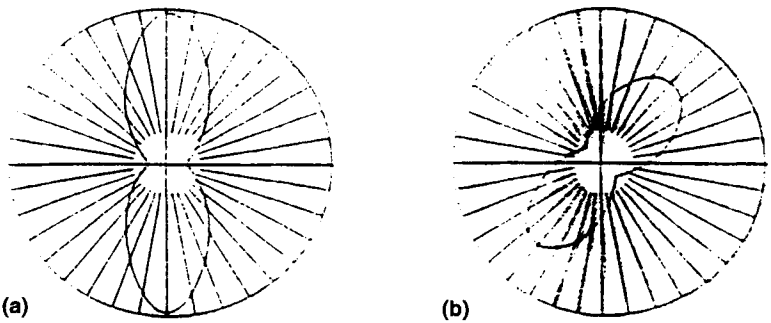

FIGURE 22 UV polarization absorption diagram of an azo PLC (a) before and (b) after the irradiation with polarized light, showing the reorientation of the optical axis [17].

Ordinary reaction kinetics has to be extended by the angular dependence of the excitation rate, and a transfer function $F(\Omega',\Omega)$ that describes the rotational diffusion during a isomerization step. The resulting equations have the form

$$\frac{df_{cis}(\Omega)}{dt} = k_1 \int F(\Omega'.\Omega) \cdot f_{trans}(\Omega') \cdot \cos^2\varphi \cdot d\Omega' - k_2 \cdot f_{cis}(\Omega) \cdot \cos^2\varphi \tag{45}$$

and can be solved numerically.

Another approach is what we call "Monte Carlo Kinetics" [76]. The system is modelled as an array of chromophore cells, each of which is described by an orientational angle and the state "*cis*" or "*trans*". The transition and orientation probabilities are determined by an adapted random process. The great advantage of a statistical modelling of the process is that there is a direct access to the implementation of the influence of absorption (penetration depth) or neighbour interactions. Figure 23 shows the simulated time evolution of the orientation parameters and the *cis* content for an ordered system.

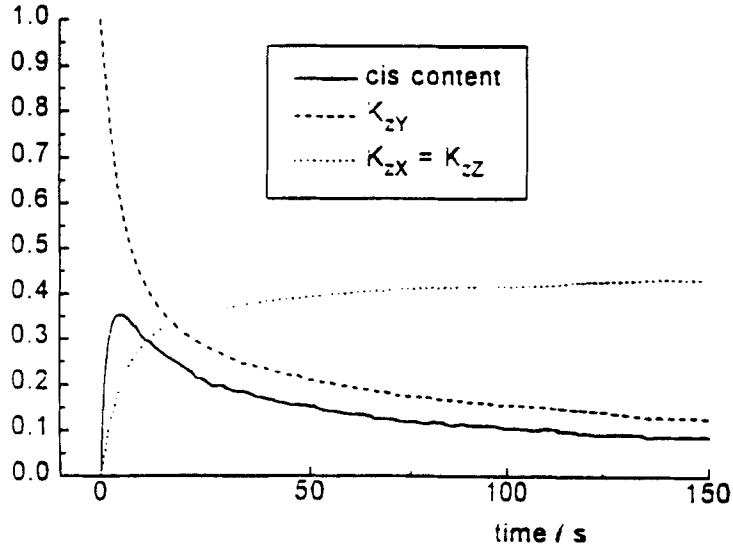

FIGURE 23 Simulated time evolution of the orientation factors K_{zX}, K_{zY} and K_{zZ} and the *cis* concentration for an oriented system with isomerizable chromophores when irradiated with *Y*-polarized light [19].

3.3.3. Investigated Systems

The first systems that have been used for this type of storage were (a) a homopolymer containing *p*-cyanoazobenzene attached to a polycarbonate [52] and (b) acrylate copolymers containing *p*-cyanoazobenzene and *p*-cyanophenyl-benzoate side chains (Fig. 24) [53].

The PLCs, having been oriented in-plane on polyimide coated glass substrates, showed an order parameter of $S = 0.71$ (for $x = 1.0$). The degree of orientation after the irradiation procedure, measured by UV dichroism, was less ($S = 0.56$), with a new direction of the optical axis. The polymers were applied for digital and holographic storage, having a very high spatial resolution (5000 lines/mm), high diffraction efficiencies ($\eta \geq 50\%$) and a low required writing intensity ($J \geq 1\,\mathrm{mW/cm^2}$) [28, 77, 78]. For these systems, the local variation of birefringence is substantially larger than 10^{-2}. Erasure can be done by heating above the clearing point or by irradiating with unpolarized or circular polarized light, while direct overwriting is done by light with a different plane of polarization. The suitability of these PLCs for polarization holography has been demonstrated.

The same type of copolymers have been investigated also by other groups. The relaxation behaviour of the photoinduced refractive index change was evaluated in detail by Wiesner *et al.* [79]. They found two relaxation processes, a relative fast one with a large relaxation time distribution, which can be described by a Williams-Watts function $\exp(-(t/\tau)^{\beta})$ with $\beta = 0.1 - 0.2$, and a slow one with a decay constant of about 15000 s. The first process was assigned partly to the isomerization of *cis*-molecules in a strained geometry [80, 81] and to reorientation

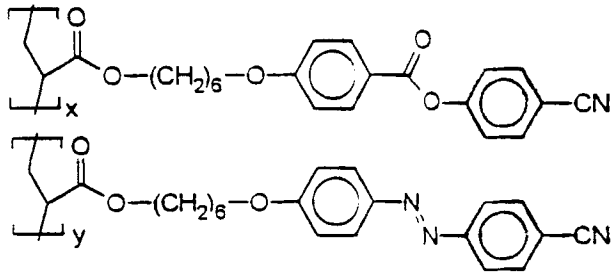

FIGURE 24 Azo copolymer used for photoorientation-based optical storage below T_g.

dynamics in the matrix, the second process corresponds to the thermal *cis-trans* isomerization in solution. The change of orientational order after irradiation was confirmed by solid state ^{13}C NMR [82].

The assignment of the relaxation processes is by no means straightforward, especially for those chromophores, where the $\pi\pi^*$ absorption band is bathochromically shifted due to donor-acceptor substitution and therefore high *cis* concentrations exist in the photostationary state. Here, one has to separate the contributions of the isomerization process and the reorientation to the sensitivity and relaxation curves. Recently we demonstrated that the isomerization of a molecule leads to almost the same change in the molecular polarizability as a reorientation; therefore the effects on the refractive index change are supposed to be of the same order of magnitude [83].

The storage properties of *homeotropically aligned* PLCs have been studied for azo copolymers with amide and biphenyl mesogenic components [84, 85]. Here, the orientation changes under irradiation from homeotropic to planar. A maximal value of $\Delta n = 0.07$ was achieved for a amide-containing copolymer at a temperature of 30°C above T_g. In the glassy state the writing process is slower, the values of Δn lower by one order of magnitude. Planar prealignment of the copolymers leads to similar resuits [86].

Recently, the photoinduced orientation of azo side chains in *cholesteric* oligosiloxanes was investigated [87, 88]. In cholesteric phases with helically aligned azo side chains, irradiation with unpolarized, linearly or circularly polarized light leads to different textures. With unpolarized or circularly polarized light a uniaxial homeotropic structure is preferred, whereas linearly polarized light orients the chromophores to a planar nematic structure.

Other investigation show that it is even possible to generate *circular birefringence* by irradiating a sample with circularly polarized light [89].

In all cases, both the polarization state of the irradiating light and the previous orientational order of the system determine the development of the molecular orientations; generally the system is biaxial. In this context, it should be pointed out that in LC cells the polarization of the light may be influenced by the cell assembly. For instance, Pfaadt *et al.*, observed by measuring the order parameters in X, Y and Z direction that an aligned azo PLC behaves not as an uniaxial system due to depolarizing effects of the aligning polyimide layer [90].

Nowadays, many groups are developing new azo polymers for the photoorientational storage. The influence of the following important parameters on the storage properties of the azo PLCs are subjects of investigation:

- **the choice of the main chain** Polyacrylates and -methacrylates [53, 77], polysiloxanes [91], polycarbonates [52] and aliphatic polyesters [92–94] have been investigated. Thus, the mechanical and thermodynamical properties of the system can be adapted to technical requirements (free standing films by polyesters and methacrylates, easy erasing by low-T_g siloxanes *etc.*).
- **the spacer** (from two to six carbon units) [86]. By the introduction of shorter spacers, amorphous azo polymers can be made which have many advantages in the preparation of optically transparent, non-scattering samples (see below).
- **the chromophore** A large variety of azo substitution can be found in literature. In most cases, the chromophore is connected to the spacer by an ethre or amino bridge (donor type). By changing the *p*-substitution of the other side of the chromophor, donor/donor or donor/acceptor dyes are realized. In particular. Disperse Red 1 and *p*-cyano substituted dyes are very popular [95, 96].
- **the mesogenic component** (azo homopolymers and copolymers with aromatic esters or amides [84, 85], biphenyles, or different chromophores).
- **the corresponding copolymer ratio** [79].
- **the molecular weight.**

All parameters influence the molecular reaction rates (*i.e.*, the photochemical *trans-cis* and *cis-trans* and the thermal *cis-trans* isomerization) and the matrix properties. The isomerization rates for various side chain polymers are given in Refs. [80, 97]. Generally, fast isomerization rates and adaption to long wavelengths are generally obtained with the donor-acceptor substituted azo chromophores ("pseudo stilbenes") [74]. The possibility of accelerating the thermal isomerization by acid catalysis was also demonstrated [98].

Long-time stability, erasability, and rewritability are very important parameter for the materials. Ramanujam and coworkers investigated the thermal behaviour of LC polyesters and found that erasing takes place at a temperature much higher than T_g [94]. They proved that it is

possible to perform 10,000 write, read and erase cycles in these azo PLCs [99].

3.3.4. Photoorientation and Surface Morphology

Very important is the question if the photoorientation process has a certain influence on the surface structure of the samples. In this case, interpretations of holographic experiments have to take surface gratings into account. Indeed, surface relief gratings with a depth modulation of more than 0.1 μm have been observed by atomic force microscopy [100, 101]. In one case, a modulation depth of 1.0 μm in a 1.2 μm thick film was measured, indicating a large mass transport during the irradiation period. After a few hours, the surface relief may disappear [102]. Nevertheless, the birefringence of the bulk is not influenced by the surface structure. The dependence of surface gratings on the polarization state in polarization holography is documented as well [103].

3.3.5. Cooperative Motion?

For a copolymer containing *p*-cyanophenyl-benzoate and *p*-methoxy-azobenzene side chains it could be shown that the co-mesogenic side chains follow the reorientation of the azo chromophore only when the irradiation has been done in the fluid liquid crystalline state [104]. Below T_g, the orientation of the benzoate mesogens remains the same, only the azo chromophores take part in the reorientation process. Thus, molecular adressing was proposed. But other investigations showed that this is not generally true: Cooperative motion even in the glassy state was demonstrated for methacrylates with *p*-unsubstituted azobenzene and *p*-methoxyphenyl-benzamide mesogenes [84] and for acrylates with *p*-cyanoazobenzene and *p*-cyanophenyl-benzoate [105, 106]. Obviously, the choice of azo dye and mesogenic unit influences the cooperative effect. Since the order parameters of both units may be different, they have to be measured separately. This can be done for instance by detecting the UV dichroism of the azo band and the IR dichroism of the CN stretching vibration, for instance. By these method, even effects on the orientation of C=O dipoles in the main chain have been detected [107].

3.3.6. A Gain Effect

The cooperative effect in PLCs leads to a very impressive gain effect. Wuttke *et al.*, showed that if a grating was written into a sample in the glassy state, and after that the temperature is increased above T_g, the diffraction efficiency is *amplified by one order of magnitude*. As th etemperature approaches the clearing point, the grating disappears. That means that the photoinduced order can be stabilized significantly by annealing; neighbouring side chains can relax into energetically favoured orientations. Although this effect uses an additional thermal treatment step, it may be very useful for the application [15].

3.3.7. Is Liquid-crystallinity Necessary?

The storage mechanism implies that in principle also amorphous polymers with photochromic moieties should be suitable for optical storage. In this case, not a reorientation of the optical axis, but photoinduced anisotropy should be observed. Actually, this behaviour was demonstrated for azo copolymers with 25% chromophore moieties, but with a very low degree of order [77]. A systematic investigation of amorphous systems began with the introduction of azo functionalized acrylates with C2 spacer units by Natansohn *et al.* [108]. It was demonstrated that the cooperative effect is not limited to PLCs [109 – 111]. The photoinduced birefringence *per azo unit* in copolymers is enhanced with respect to the corresponding homopolymers, but normally does not exceed the absolute value. We showed that the correlations between the different side chains are both of first order (dipolar interactions) as well as of second order (form anisotropy), even in amorphous polymers [112]. Of special interest are copolymers that are on the border to liquid crystallinity, bearing rigid side groups with a high anisotropy of geometrical shape and molecular polarizability. They exhibit very high values of photoinduced birefringence (*e.g.*, for the polymer in Figure 25 $\Delta n = 0.08$ with an order parameter $S = 0.14$) [110].

Amorphous films can also be obtained from PLCs by fast cooling from the isotropic melt to the glassy state, avoiding the alignment process [16, 113]. The resulting films are optically clear and exhibit high values of photoinduced birefringence and dichroism. A prealignment can also be avoided by direct spin-coating the PLCs onto a substrate.

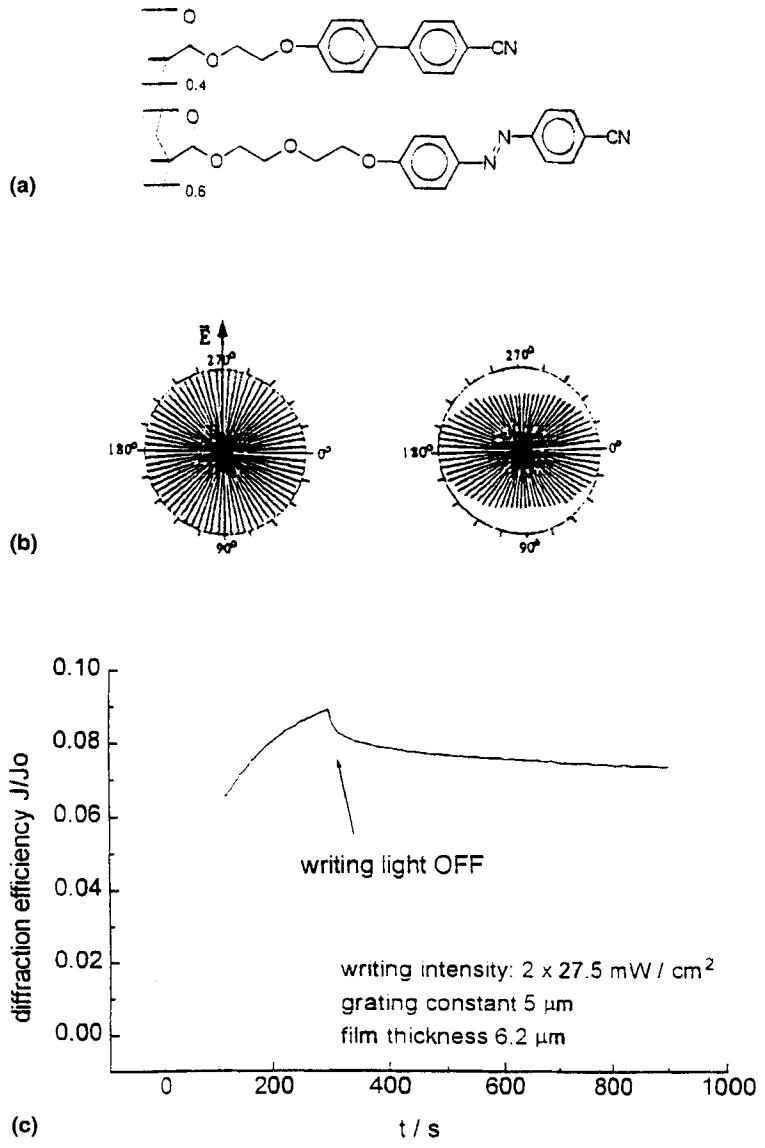

FIGURE 25 (a) An amorphous copolymer, in which high birefringence can be induced by polarized light; (b) IR polar diagram (CN stretching band) before and after irradiation [110] (reproduced with permission); (c) Holographic growth and relaxation curve (unpublished results).

For instance, anisotropic films of polyesters with high molecular weight, which are able to form free-standing films, were made by this way [92].

Because of their advantages in preparation, it is to be expected that amorphous films have a greater chance for a possible application in optical storage than oriented PLCs.

3.3.8. LB Monolayers

Besides bulk liquid crystalline and amorphous phases'. Langmuir Blodgett (LB) films are the third type of materials that have been investigated with respect to photoinduced reorientation mechanisms. For instance, LB films of cholesteric polyacrylates [114 – 117] and "hairy rod" polyglutamates [42, 118 – 120] combining amphiphilic and thermotropic properties were prepared. These polymers form mono- and multilayer structures with a parallel arrangement of the azo side chains. Under UV irradiation, the *trans-cis* isomerization destroys the alignment of the rigid *trans* azo groups. This destruction of the LB film order corresponds to the isothermal LC-isotropic phase transition described in Section 3.1. Controlled irradiation with polarized light leads to in-plane anisotropic structures, so that the concept of photoorientation seems also to be applicable. However, there are some differences in the mechanism because of energy dissipation and the collectivity of the rearrangement, so the mechanism lies somewhere between photoorientation and phase transition [121].

Related systems are monomolecular amphiphiles [122, 123] and non-amphiphilic LB films [124], the latter having been prepared by a processor method. The latter system contains azo groups lying in random orientation onto the surface of the film, and they can be oriented totally in-plane.

3.3.9. Photoelectrochemical Systems

The photoisomerization reaction of azobenzene may be coupled to an electrochemical reaction. When the hydrophilic part of an LB layer with pendant azo groups is in contact with a reducing aqueous solution, the *cis* isomers of azo molecules can be selectively reduced to the hydrazo form. Thus, the system consists of a three-state cycle (Fig. 26). The application of those hybride systems with respect to high density storage [125], and the possibility of polarization-dependent processes

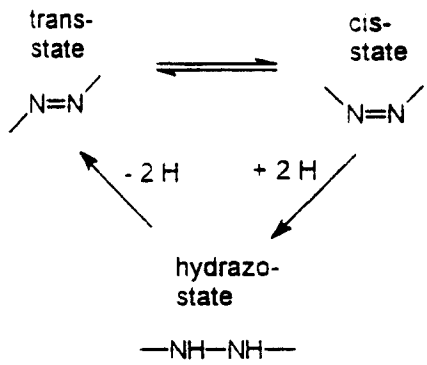

FIGURE 26 The electrochemical reduction cycle of azo dyes [125].

[126] have been investigated. To azo PLCs, however, it has not been applied yet.

3.3.10. Electric Field Assisted Photoorientation

Furthermore, the combination of the photoreorientation mechanism with electric field effects gives rise to interesting questions: (a) Can the photoorientation process be accelerated by an external electric field and (b) can the chromophore be poled? While there are no hints for an acceleration effect, the possibility of poling was demonstrated for the controlled photoorientation in cholesteric PLCs [87, 127, 128] as well as in LB films by applying a dc field both in-plane and out-of-plane respectively [129]. Very interesting from the point-of-view of all-optical systems is the fact that poling can also be done in a pure optical way by the superposition of the writing light with its second harmonic [130]. The main application, however, of these poled systems lies in the field of NLO materials for second harmonic generation and not in optical storage. A review about poling and photoorientation including molecular guest-host systems can be found in Ref. [99].

3.3.11. Stilbenes and Other Dyes

The question arises if there are other photostationary systems that can be used for the photoreorientation mechanism. Indanedione and benzofuranone dyes were investigated , but they showed no significant effect [131]. Stilbenes are very similar to azo dyes, but they easily

undergo ring closure and subsequent oxidation to phenanthrene. In order to find stable stilbenes that would stand many isomerization cycles, this reaction must be prevented. A solution of this problem are benzylidenindanes (Fig. 27). Incorporated into cholesteric polysiloxanes, we presented them recently as high-efficient recording media at UV wavelengths [76, 132, 133]. Because of their transparency, they find applications not mainly in optical storage, but, for instance, as reconfigurable holographic optical elements with the possibility of fine

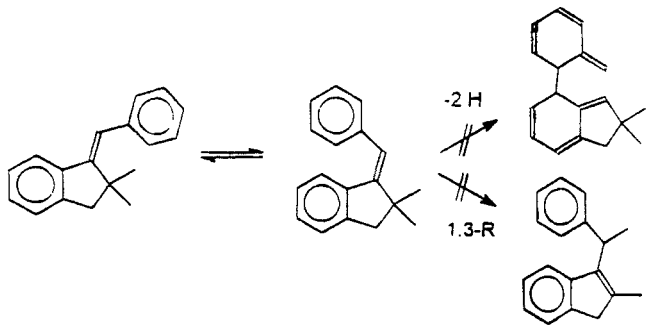

FIGURE 27 A stilbene derivative which can be used for optical storage in the UV region. Because of its substitution, it is inert with respect to oxidative ring closure and 1,3-alkyl shift [131].

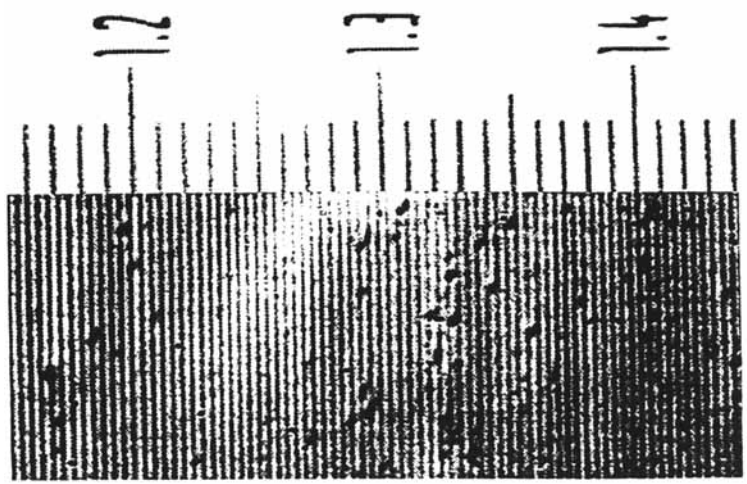

FIGURE 28 Diffraction grating recorded in a LC stilben oligosiloxane (polarizing microscopy).

tuning the refractive index properties. Figure 28 displays a grating structure written into a stilbene oligosiloxane, viewed in a polarizing microscope.

3.3.12. Further Applications: Command Surfaces

The photoorientation process has applications that go beyond the use as optical memory systems. For instance, the alignment of liquid crystals in display cells by the means of photocontrolled command layers [134] offers very interesting applications in display technology and optical signal processing. The principle has been investigated mainly in Japan, by Ichimura *et al.* The command layers are azobenzene moieties which are directly attached to the glass surface of a electrooptical cell [135, 136]. The alignment of MLCs in these cells can be switched reversibly between homeotropic and homogenous by alternate exposure to UV and visible light. Three dimensional control of the molecular orientation has been achieved by irradiation with polarized light. In principle, all azo polymers are suitable for command surfaces, but it was pointed out, that perfect switching between different directions in the planar state should be done with laterally attached azobenzenes (Fig. 29). Thus, command surface polymers with the azo group working as a "molecular rotor" have been developed [137, 138].

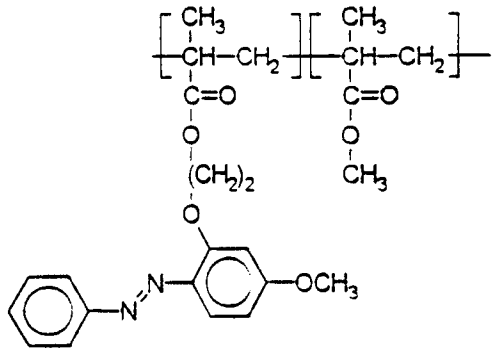

FIGURE 29 A "molecular rotor" which has been applied as a command surface for the alignment of MLC's. [138].

3.4. Photopolymerizable Systems

Finally, a system should be presented that uses a rather different mechanism for optical storage: the polymerization of the liquid-crystalline precursor monomers [139, 140]. The system consists of a LC monomer, doped with a polar MLC (20%) and a photoinitiator. The sample film is held between glass plates that have been coated with indium tin oxide electrodes and a rubbed layer of polyimide. Holographic gratings can be written at 488 nm by crosslinking the monomers (Fig. 30). The resulting variation of the refractive index immediately after the writing process is small. In a conventional photopolymer, diffusion of the monomer into the polymeric regions and subsequent irradiation of the whole sample area would give the final refractive index modulation. Here, the switching properties of liquid crystals in an electric field can be used, and the diffraction efficiency is enhanced by applying an ac field (3V), because the monomers in the unirradiated areas align homeotropically. The switching is reversible: when the field is shut off, planar alignment is preferred. In a last step, fixing can be done by irradiating the whole area. Thus, gain factors of 8000 for the diffraction efficiency were achieved by applying the electric field. The minimum switching time was reported to be ≤ 33 ms; after 10^5 switching cycles 7% degradation was observed.

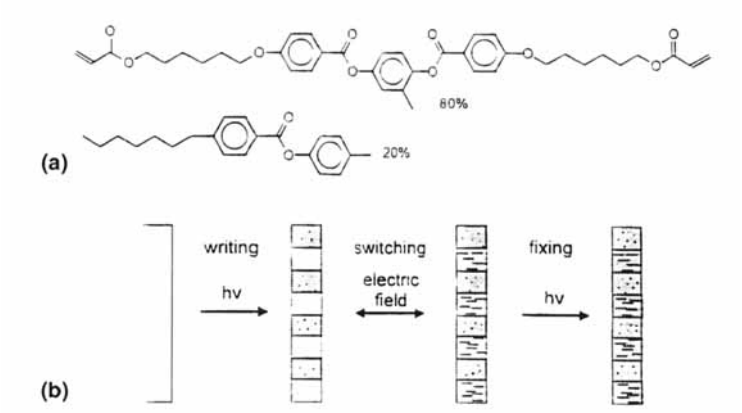

FIGURE 30 (a) Compounds for optical storage *via* photopolymerization; (b) Storage principle for the photopolymer system. The alignment in the monomeric regions can be switched by applying an electric field (redrawn from [140]).

4. OUTLOOK

Various mechanisms can be used for realizing optical storage in PLCs. Among the different systems, azo PLCs seem to be the most promising polymers for future applications, either with the phase-transition or the photoreorientation mechanism. Still there are some problems: the sensitivity of the systems has to be enhanced if they should be suitable for digital or holographic storage systems. Nevertheless, they have great advantages due to their easy processability, the stability of the stored information and the reversibility of the storage.

In this paper we have covered only the optical properties that can be controlled by light, but the concept of switching polymer properties by light [141] can be extended also to other applications: for azo side chain polymers the influence of the light-induced isomerization on the ion conductivity of the polymers [142], the solubility [143] and the dielectric properties [144] has been investigated, for instance. Of special interest with respect to optical storage is the possibility of switching the polarization in ferroelectric LC phases by photochromic compounds [145].

Today, many research groups are working on optical switching devices that are based on these or related systems, and it has to be expected that there will be interesting new ideas in the future.

References

[1] Emmeiius, M., Pawlowski, G. and Vollmann, H. (1989). *Angew. Chem.*, **101**, 1475.
[2] Johnson, G., Thomas, G. and others (1989). In: *Ullman's Encyclopedia of Industrial Chemistry A14*, 5th edn. (Eds. Elvers, B. and Gerhartz, W.). VCH, Weinheim. Basel, Cambridge, New York, p. 171.
[3] Kaempf, G. and Mergel, D. (1995). In: *Kirk-Othmer Encyclopedia of Chemical Technology*, 4th edn. Vol. 14, Wiley, New York, p. 277.
[4] Schwartz, K. (1995). The Physics of Optical Recording, Springer-Verlag, Berlin, Heidelberg, New York.
[5] Gabor, D. (1948). *Nature*, **161**, 777.
[6] Hariharan, P. (1984). Optical holography, Cambridge University Press, Cambridge.
[7] Heanue, J., Bashaw, M. and Hesselink, L. (1994). *Science*, **265**, 749.
[8] Smith, H. (Ed.) (1997). Holographic Recording Materials, Springer-Verlag, Berlin. Heidelberg, New York.
[9] Solano, C. (1994). *Rev. Mex. Fisica*, **40**, 686.
[10] Caulfield, H. (Ed.) (1979). Handbook of Optical Holography, Academic Press.
[11] Braeuchle, C. and Burland, D. (1983). *Angew. Chemic*, **95**, 612.
[12] Burland, D. and Braeuchle, C. (1982). *J. Chem. Phys.*, **76**, 4502.

[13] Eichler, H., Guenter, P. and Pohl, D. (1986). Laser-induced Dynamic Gratings, Springer-Verlag, Berlin. Heidelberg.
[14] Kogelnik, H. (1969). *Bell Syst. Tech. J.*, **48**, 2909.
[15] Wuttke, R. (1994). *Ph.D. Thesis*, Univ. Bayreuth.
[16] Bieringer, T., Wuttke, R. and Haarer, D. (1995). *Macromol. Chem. Phys.*, **196**, 1375.
[17] Anderle, K. (1995). *Ph.D. Thesis*, Univ. Marburg.
[18] Jena, A. V. and Lessing, H. (1979). *Optical Quantum Electronics*, **11**, 419.
[19] Fuhrmann, T. (1997). *Ph.D. Thesis*, Univ. Marburg.
[20] Rokushima, K. and Yamakita, J. (1983). *J. Opt. Soc. Am.*, **73**, 901.
[21] Johnson, R. V. and Tanguay, A. R. (1986). *Optical Engineering*, **25**, 235.
[22] Vachss, F. and Hesselink, L. (1987). *J. Opt. Soc. Am. A*, **4**, 325.
[23] Glytsis, E. N. and Gaylord, T. K. (1987). *J. Opt. Soc. Am. A*, **4**, 2061.
[24] Huang, T. and Wagner, K. (1996). *J. Opt. Soc. Am. B*, **13**, 282.
[25] Kakichasvili, S. (1972). *Optics & Spectroscopy*, **33**, 171.
[26] Todorov, T., Nikolova, L. and Tomova, N. (1984). *Appl. Opt.*, **23**, 4588.
[27] Nikolova, L. and Todorov, T. (1984). *Optica Acta*, **31**, 579.
[28] Anderle, K. and Wendorff, J. (1994). *Mol. Cryst. Liq. Cryst.*, **243**, 51.
[29] Jones, R. (1941). *J. Opt. Soc. Am.*, **31**, 488.
[30] Fourkas, J., Trebino, R. and Fayer, M. (1992). *J. Chem. Phys.*, **97**, 69.
[31] Michl, J. and Thulstrup, E. (1986). Spectroscopy with Polarized Light, VCH, New York.
[32] Samori, B. and Thulstrup, E. (Eds.) (1988). Polarized Spectroscopy of Ordered Systems, Kluwer Academic Publishers, Dordrecht, Boston. London.
[33] Zeisel, D. (1993). *Ph.D. Thesis*, Uni. Muenchen
[34] Jungnickel, B.-J. and Wendorff, J. (1991). In: *Chemistry and Physics of Macromolecules*. (Ed. Deutsche Forschungs-Gemeinschaft), VCH, Weinheim. p. 349.
[35] Fredericq, E. and Houssier, C. (1973). Electric dichroism and electric birefringence, Clarendon Press, Oxford.
[36] Gear, J., Goodby, J., Kmetz, A. and Patel, J. (1987). *J. Appl. Phys.*, **62**, 4100.
[37] Ulrich, R. and Torge, R. (1973). *Appl. Opt.*, **12**, 2901.
[38] Morino, S., Machida, S., Yamashita, T. and Horie, K. (1995). *J. Phys. Chem.*, **99**, 10280.
[39] Andrews, J. and Singer, K. (1993). *Appl. Opt.*, **32**, 6703.
[40] Warenghem, M. and Grover, C. (1988). *Mol. Cryst. Liq. Cryst.*, **159**, 15.
[41] Azzam, R. and Bashara, N. (1977). Ellipsometry and Polarized Light, North-Holland, Amsterdam.
[42] Hickel, W., Dude, G., Wegner, G. and Knoll, W. (1989). *Makromol. Chem. Rapid. Commun.*, **10**, 353.
[43] McArdle, C. (1989). In: *Side Chain Liquid Crystal Polymers*, (Ed. McArdle, C.), Blackie, Glasgow. London.
[44] Shibaev, V., Kostromin, S., Plate, N., Ivanov, S., Vetrov, V. and Yakovlev, I. (1983). *Polym. Commun.*, **24**, 364.
[45] Sasaki, A. (1986). *Mol. Cryst. Liq. Cryst.*, **139**, 103.
[46] Coles, H. and Simon, R. (1985). *Polymer*, **26**, 1801.
[47] McArdle, C., Clark, M., Haws, C., Wiltshire, M., Parker, A., Nestor, G., Gray, G., Lacey, D. and Toyne, K. (1987). *Liq. Cryst.*, **2**, 573.
[48] Schmidt, H. (1989). *Angew. Chem. Adv. Mater.*, **101**, 964.
[49] Griffin, A., Hoyle, C., Gross, J., Venkataram, K., Creed, D. and McArdle, C. (1988). *Makromol. Chem. Rapid Commun.*, **9**, 463.
[50] Nakamura, T. and Ueno, T., *Proc. of 12th Japanese Symp. on Liq. Cryst.*
[51] Nakamura, T., Ueno, T. and Tani, C. (1989). *Mol. Cryst. Liq. Cryst.*, **169**, 167.
[52] Eich, M., Wendorff, J., Reck, B. and Ringsdorf, H. (1987). *Makromol. Chemic. Rapid Commun.*, **8**, 59.
[53] Eich, M. and Wendorff, J. (1987). *Makromol. Chem. Rapid Commun.*, **8**, 467.

[54] Ikeda, T., Horiuchi, S., Karanjit, D., Kurihara, S. and Tazuke, S. (1990). *Macromolecules*, **23**, 36.
[55] Ikeda, T., Horiuchi, S., Karanjit, D., Kurihara, S. and Tazuke, S. (1990). *Macromolecules*, **23**, 42.
[56] Ikeda, T., Kurihara, S., Karanjit, D. and Tazuke, S. (1990). *Macromolecules*, **23**, 3938.
[57] Ikeda, T., Miyamoto, T., Kurihara, S. and Tazuke, S. (1990). *Mol. Cryst. Liq. Cryst.*, **188**, 223.
[58] Ikeda, T., Miyamoto, T., Sasaki, T., Kurihara, S. and Tazuke, S. (1990). *Mol. Cryst. Liq. Cryst.*, **188**. 235.
[59] Nakamura, K., Kikuchi, H. and Kajiyama, T. (1994). *Polym. J.*, **26**, 1090.
[60] Kato, T., Hirota, N., Fujishima, A. and Frechet, J. (1996). *J. Polym. Sci. A*, **34**, 57.
[61] Pinsl, J., Braeuchle, C. and Kreuzer, F. (1987). *J. Molec. Electron.*, **3**, 9.
[62] Boiko, N., Kutulya, L., Reznikov, Y., Sergan, T. and Shibaev, V. (1994). *Mol. Cryst. Liq. Cryst.*, **251**, 311.
[63] Narisawa, H., Kishi, R. and Sisido, M. (1995). *Macromol. Chem. & Phys.*, **196**, 1419.
[64] Chung, D., Kim, J., Min, K. and Park, K. (1995). *Mol. Cryst. Liq. Cryst. A*, **267**, 399.
[65] Feringa, B., Jager, W. and DeLange, B. (1993). *Tetrahedron*, **49**, 8267.
[66] Cabrera, I., Krongauz, V. and Ringsdorf, H. (1987). *Angew. Chem. Int. Ed. Engl.*, **26**, 1178.
[67] Yitzchaik, S., Cabrera, I., Buchholtz, F. and Krongauz, V. (1990). *Macromolecules*, **23**, 707.
[68] Natarajan, L., Tondiglia, V., Bunning, T., Crane, R. and Adams, W. (1992). *Adv. Mater. Opt. Electron.*, **1**, 293.
[69] Cabrera, I., Dittrich, A. and Ringsdorf, H. (1991). *Angew. Chem.*, **103**, 106.
[70] Darcy, P., Heller, H., Strydom, P. and Whittall, J. (1981). *Perkin Trans. I*, p. 202.
[71] Ramanujam, P., Hvilsted, S. and Andruzzi, F. (1993). *Appl. Phys. Lett.*, **62**, 1041.
[72] Ramanujam, P., Hvilsted, S., Zebger, I. and Siesler, H. (1995). *Macromol. Rapid. Commun.*, **16**, 455.
[73] Bach, H., Anderle, K., Fuhrmann, T. and Wendorff, J. (1995). *J. Phys. Chem.*, **100**, 4135.
[74] Rau, H. (1988). In: *Photochemistry and Photophysics*. (Ed. Rabek, J.), CRC Press, Boca Raton, FLchapter II, p. 4.
[75] Birenheide, R. (1991). *Ph.D. Thesis*, TH Darmstadt.
[76] Fuhrmann, T., Kunze, M., Lieker, I., Stracke, A. and Wendorff, J. H. (1996). *Proc. SPIE*, **2852**.
[77] Anderle, K., Birenheide, R., Eich, M. and Wendorff, J. (1989). *Makromol. Chem., Rapid Commun.*, **10**, 477.
[78] Eich, M. and Wendorff, J. (1990). *J. Opt. Soc. Am. B*, **7**, 1428.
[79] Wiesner, U., Antonietti, M., Boeffel, C. and Spiess, H. (1990). *Makromol. Chem.*, **191**, 2133.
[80] Paik, C. and Morawetz, H. (1972). *Macromolecules*, **5**, 171.
[81] Eisenbach, C. (1978). *Makromol. Chem.*, p. 2489.
[82] Wiesner, U., Schmidt-Rohr, K., Boeffel, C., Pawelzik, U. and Spiess, H. (1990). *Adv. Mater.*, **2**, 484.
[83] Kunze, M. (1996). *Master's Thesis*, Univ. Marburg.
[84] Stumpe, J., Mueller, L., Kreysig, D., Hauck, G., Koswic, H., Ruhmann, R. and Ruebner, J. (1991). *Makromol. Chem., Rapid Commun.*, **12**, 81.
[85] Ivanov, S., Yakovlev, I., Kostromin, S., Shibaev, V., Laesker, L., Stumpe, J. and Kreysig, D. (1991). *Makromol. Chem., Rapid Commun.*, **12**, 709.
[86] Fischer, T., Laesker, L., Stumpe, J. and Kostromin, S. (1994). *J. Photochem. Photobiol. A*, **80**, 453.
[87] Petri, A., Kummer, S., Anneser, H., Feiner, F. and Braeuchle, C. (1993). *Ber. Bunsenges. Phys. Chem.*, **97**, 1281.
[88] Petri, A., Kummer, S. and Braeuchle, C. (1995). *Liq. Cryst.*, **19**, 277.

[89] Nikolova, L., Todorov, T., Ivanov, M., Andruzzi, F., Hvilsted, S. and Ramanujam, P. (1996). *Appl. Opt.*, **35**, 3835.
[90] Pfaadt, M., Boeffel, C. and Spiess, H. (1996). *Acta Polymer*, **47**, 35.
[91] Ortler, R., Braeuchle, C., Millera, A. and Riepl, G. (1989). *Markromol. Chem. Rapid Commun.*, **10**, 189.
[92] Hvilsted, S., Andruzzi, F. and Ramanujam, P. (1992). *Opt. Lett.*, **17**, 1234.
[93] Hvilsted, S., Andruzzi, F., Kulinna, C., Siesler, H. and Ramanujam, P. (1995). *Macromolecules*, **28**, 2172.
[94] Holme, N., Ramanujam, P. and Hvilsted, S. (1996). *Appl. Opt.*, **35**, 4622.
[95] Zebger, I., Kulinna, C., Siesler, H., Andruzzi, F., Pedersen, M., Ramanujam, P. and Hvilsted, S. (1995). *Macromol. Symp.*, **94**, 159.
[96] Ho, M., Natansohn, A., Barrett, C. and Rochon, P. (1995). *Can. J. Chem.*, **73**, 1773.
[97] Barrett, C., Natansohn, A. and Rochon, P. (1995). *Chem. Mater.*, **7**, 899.
[98] Haitjema, H., Tan, Y. and Challa, G. (1995). *Macromolecules*, **28**, 2867.
[99] Holme, N., Ramanujam, P. and Hvilsted, S. (1996). *Opt. Lett.*, **21**, 902.
[100] Kim, D., Li, L., Jiang, X., Shivshankar, V., Kumar, J. and Tripathy, S. (1995). *Macromolecules*, **28**, 8835.
[101] Barrett, C., Natansohn, A. and Rochon, P. (1996). *J. Phys. Chem.*, **100**, 8836.
[102] Ramanujam, P., Holme, N. and Hvilsted, S. (1996). *Appl. Phys. Lett.*, **68**, 1329.
[103] Jiang, X., Kumar, J., Kim, D., Shivshankar, V. and Tripathy, S. (1996). *Appl. Phys. Lett.*, **68**, 2618.
[104] Anderle, K., Birenheide, R., Werner, M. and Wendorff, J. (1991). *Liq. Cryst.*, **9**, 691.
[105] Wiesner, U., Reynolds, N., Boeffel, C. and Spiess, H. (1991). *Makromol. Chem. Rapid Commun.*, **12**, 457.
[106] Wiesner, U., Reynolds, N., Boeffel, C. and Spiess, H. (1992). *Liq. Cryst.*, **11**, 251.
[107] Buffeteau, T. and Pezolet, M. (1996). *Appl. Spectr.*, **50**, 948.
[108] Natasohn, A., Rochon, P., Gosselin, J. and Xie, S. (1992). *Macromolecules*, **25**, 2268.
[109] Natansohn, A., Rochon, P., Pezolet, M., Audet, P., Brown, D. and To, S. (1994). *Macromolecules*, **27**, 2580.
[110] Laesker, L., Fischer, T., Stumpe, J., Kostromin, S., Ivanov, S., Shibaev, V. and Ruhmann, R. (1994). *Mol. Cryst. Liq. Cryst.*, **246**, 347.
[111] Meng, X., Natansohn, A., Barrett, C. and Rochon, P. (1996). *Macromolecules*, **29**, 946.
[112] Stracke, A. (1996). *Master's Thesis*, Univ. Marburg.
[113] Laesker, L., Fischer, T., Stumpe, J., Kostromin, S., Inanov, S., Shibaev, V. and Ruhmann, R. (1994). *Mol. Cryst. Liq. Cryst.*, **253**, 1.
[114] Ringsdorf, H., Urban, C., Knoll, W. and Sawodny, M. (1992). *Makromol. Chem.*, **193**, 1235.
[115] Sawodny, M., Schmidt, A., Reiter, G., Stamm, M., Knoll, W., Urban, C. and Ringsdorf, H. (1991). *Polym. Adv. Technol.*, **2**, 127.
[116] Moebius, G., Pietsch, U., Geue, T., Stumpe, J., Schuster, A. and Ringsdorf, H. (1994). *Thin Solid Films*, **247**, 235.
[117] Geue, T., Stumpe, J., Pietsch, U., Haak, M. and Kaupp, G. (1995). *Mol. Cryst. Liq. Cryst. A*, **262**, 157.
[118] Menzel, H. and Weichart, B. (1994). *Thin Solid Films*, **242**, 56.
[119] Sekkat, Z., Buechel, M., Orendi, H., Menzel, H. and Knoll, W. (1994). *Chem. Phys. Lett.*, **220**, 497.
[120] Menzel, H., Weichart, B., Schmidt, A., Paul, S., Knoll, W., Stumpe, J. and Fischer, T. (1994). *Langmuir*, **10**, 1926.
[121] Schoenhoff, M., Mertesdorf, M. and Loesche, M. (1996). *J. Phys. Chem.*, **100**, 7558.
[122] Schoenhoff, M., Chi, L., Fuchs, H. and Loesche, M. (1995). *Langmuir*, **11**, 163.
[123] Gillberg, G., Leube, H., McKenzie, L., Pruksarnukul, L. and Reeder, L. (1994). *J. Appl. Polym. Sci.*, **53**, 687.

[124] Yokohama, S., Kakimoto, M. and Imai, Y. (1994). *Thin Solid Flims*, 1992, **242**, 183.
[125] Liu, Z., Hashimoto, K. and Fujishima, A. (1992). *AIP Conf. Proc.*, 1992, **262**, 218.
[126] Wang, R., Iyoda, T., Hashimoto, K. and Fujishima, A. (1995). *J. Phys. Chem.*, **99**, 3352.
[127] Anneser, H., Feiner, F., Petri, A., Braeuchle, C., Leigeber, H., Weitzel, H.-P., Kreuzer, F.-H., Haak, O. and Boldt, P. (1993). *Adv. Mater.*, **5**, 556.
[128] Dietrich, R., Kastenmueller, G., Bourhill, G., Braeuchle, C., Leigeber, H., Weitzel, H. and Kreuzer, F. (1996). *Ber. Bunsenges. Phys. Chem.*, **100**, 1128.
[129] Palto, S., Blinov, L., Yudin, S., Grewer, G., Schoenhoff, M. and Loesche, M. (1993). *Chem. Phys. Lett.*, **202**, 308.
[130] Charra, F., Fiorini, C. and Nunzi, J.-M. (1994). *IEEE Proceedings*, **ISE 8**, 769.
[131] Leupold, J. (1994). *Ph.D. Thesis*, TU Braunschweig.
[132] Lieker, I. (1996). *Master's Thesis*, Univ. Marburg.
[133] Fuhrmann, T., Lieker, I., Wendorff, J. H., Zippel, S. and Boldt, P. (1996). *Freiburger Arbeitstagung Fluessigkristalle.*
[134] Gibbons, W., Shannon, P., Sun, S.-T. and Swetlin, B. (1991). *Nature*, **351**, 49.
[135] Kawanishi, Y., Tamaki, T., Sakuragi, M., Seki, T., Suzuke, Y. and Ichimura, K. (1992). *Langmuir*, **8**, 2601.
[136] Kawanishi, Y., Suzuki, Y. and Sakuragi, M. (1994). *J. Photochem. Photobiol. A: Chem.*, **80**, 433.
[137] Akiyama, H., Momose, M. and Ichimura, K. (1995). *Macromolecules*, **28**, 288.
[138] Akiyama, H., Kudo, K. and Ichimura, K. (1995). *Macromol. Rapid Commun.*, **16**, 35.
[139] Zhang, J. and Sponsler, M. (1992). *J. Am. Chem. Soc.*, **114**, 1506.
[140] Zhang, J. Carlen, C., Palmer, S. and Sponsler, M. (1994). *J. Am. Chem. Soc.*, **116**, 7055.
[141] Kumar, G. and Neckers, D. (1989). *Chem. Rev.*, **89**, 1915.
[142] Tokuhisa, H., Yokohama, M. and Kimura, K. (1994). *Macromolecules*, **27**, 1842.
[143] Kroeger, R., Menzel, H. and Hallensleben, M. (1994). *Macromol. Chem. Phys.*, **195**, 2291.
[144] Fuhrmann, T. and Wendorff, J. (1994). *Dielectric Newsletters* (*2*), 1.
[145] Ikeda, T., Sasaki, T. and Ichimura, K. (1993). *Nature*, **361**, 428.